PTEN drives Th17 cell differentiation by preventing IL-2 production

Hyeong Su Kim, Sung Woong Jang, Wonyong Lee, Kiwan Kim, Hyogon Sohn, Soo Seok Hwang, and Gap Ryol Lee

Department of Life Science, Sogang University, Seoul, South Korea

T helper 17 (Th17) cells are a CD4$^+$ T cell subset that produces IL-17A to mediate inflammation and autoimmunity. IL-2 inhibits Th17 cell differentiation. However, the mechanism by which IL-2 is suppressed during Th17 cell differentiation remains unclear. Here, we show that phosphatase and tensin homologue (PTEN) is a key factor that regulates Th17 cell differentiation by suppressing IL-2 production. Th17-specific *Pten* deletion (*Pten*$^{fl/fl}$*Il17a*^{cre}) impairs Th17 cell differentiation in vitro and ameliorated symptoms of experimental autoimmune encephalomyelitis (EAE), a model of Th17-mediated autoimmune disease. Mechanistically, *Pten* deficiency up-regulates IL-2 and phosphorylation of STAT5, but reduces STAT3 phosphorylation, thereby inhibiting Th17 cell differentiation. PTEN inhibitors block Th17 cell differentiation in vitro and in the EAE model. Thus, PTEN plays a key role in Th17 cell differentiation by blocking IL-2 expression.

The Journal of Experimental Medicine

INTRODUCTION

CD4$^+$ T cells are key components of the adaptive immune system and are indispensable for pathogen clearance and host protection. CD4$^+$ Th1, Th2, and Th17 cells are effector T cells that defend against various pathogens (Zhou et al., 2009; Zhu et al., 2010). Th17 cells produce IL-17A, IL-17F, IL-22, and other chemokines that recruit neutrophils to sites of infection and mediate clearance of pathogens such as extracellular bacteria and fungi (Zhou et al., 2009; Zhu et al., 2010). In addition, Th17 cells play a critical role in human autoimmune diseases such as multiple sclerosis and rheumatoid arthritis (Chabaud et al., 2001; Annunziato et al., 2007). Differentiation of CD4$^+$ naive T cells into Th17 cells is regulated by IL-6 and TGF-β (Bettelli et al., 2006; Mangan et al., 2006; Veldhoen et al., 2006; Chung et al., 2009; Ghoreschi et al., 2010; Kimura and Kishimoto, 2010). Upon binding to IL-6R on the cell membrane, IL-6 drives phosphorylation and dimerization of STAT3 (Korn et al., 2009). STAT3 dimers subsequently translocate to the nucleus and induce expression of transcription factor RORγt, which plays a crucial role in driving Th17 cell differentiation (Ivanov et al., 2006; Yang et al., 2008).

IL-2 plays an important role in clonal expansion of activated CD4$^+$ T cells. Activated CD4$^+$ T cells express high-affinity IL-2R, which comprises α, β, and γ chains, and at the same time produce IL-2 (Gaffen, 2001). Binding of IL-2 to IL-2R contributes to clonal expansion of CD4$^+$ T cells via activation of multiple signaling cascades such as JAK-STAT and PI3K/Akt (Lin and Leonard, 2000; Fung et al., 2003). Therefore, IL-2 is a potent growth factor for CD4$^+$ T cells. However, it has opposite effects on Th17 cells (Laurence et al., 2007; Liao et al., 2011). In these cells, IL-2 inhibits IL-6R expression and instead induces STAT5 phosphorylation, which inhibits Th17 cell differentiation (Laurence et al., 2007; Yang et al., 2011). Therefore, although IL-2 expression must be repressed to allow Th17 cell differentiation, the molecular mechanisms by which IL-2 is controlled during Th17 cell differentiation remain elusive.

PI3K/Akt signaling is a representative signaling pathway for cell survival, which is activated by IL-2, the TCR, and a costimulatory receptor (CD28; Ward et al., 1992; Fung et al., 2003). Phosphatase and tensin homologue (PTEN), a tumor suppressor, is a negative regulator of PI3K signaling. PTEN dephosphorylates phosphatidyl-3,4,5-triphosphate (PIP_3) into phosphatidyl-4,5-biphosphate (PIP_2), thereby inhibiting the PI3K signaling cascade (Maehama and Dixon, 1998). Several studies reveal that PTEN plays an important role in T cell homeostasis and functions in certain subsets of CD4$^+$ T cells (Suzuki et al., 2001; Huynh et al., 2015; Shrestha et al., 2015). For instance, *Pten*$^{fl/fl}$*Lck*^{cre} mice, which harbor T cell–specific deletion of *Pten*, show disrupted T cell homeostasis and self-tolerance (Suzuki et al., 2001). In addition, *Pten*$^{fl/fl}$ *Foxp3*^{cre} mice, which harbor regulatory T (T reg) cell–specific deletion of *Pten*, show loss of T reg cell function and stability (Huynh et al., 2015; Shrestha et al., 2015).

Here, we used Th17-specific *Pten*-deficient mice to examine the role of PTEN in Th17 cell differentiation. We found that Th17-specific deletion of *Pten* blocks Th17 cell differentiation in vitro. Mice with experimental autoimmune encephalomyelitis (EAE), a model of human multiple sclerosis

Correspondence to Gap Ryol Lee: grlee@sogang.ac.kr

Abbreviations used: cKO, conditional KO; CNS, central nervous system; EAE, experimental autoimmune encephalomyelitis; MOG, myelin oligodendrocyte glycoprotein; pLN, peripheral LN; PTEN, phosphatase and tensin homologue; qRT-PCR, quantitative RT-PCR.

The Rockefeller University Press
J. Exp. Med. 2017 Vol. 214 No. 11 3381–3398
https://doi.org/10.1084/jem.20170523

(Cua et al., 2003; Komiyama et al., 2006), show Th17-specific deletion of *Pten*, which ameliorated disease symptoms and disrupted Th17 cell differentiation. *Pten* deficiency induces IL-2 expression and STAT5 phosphorylation, but reduces STAT3 phosphorylation. Furthermore, a specific inhibitor of PTEN, SF1670 (Li et al., 2011), effectively blocks EAE development. Collectively, these results demonstrate that *Pten* acts as a key regulator of Th17 cell differentiation by regulating IL-2 expression.

RESULTS

Pten deficiency inhibits Th17 cell differentiation in vitro

To investigate the role of PTEN in Th17 cell differentiation, we first measured subset-specific expression of PTEN. We stimulated naive $CD4^+$ T cells from C57BL/6 mice under Th1-, Th2-, Th17-, and T reg–polarizing conditions and examined expression of PTEN at the RNA (Fig. 1 A) and protein levels (Fig. 1 B). PTEN expression was higher in Th17 cells than in Th1 and Th2 cells, but lower than in T reg cells. To further investigate the Th17-specific role of PTEN, we generated Th17-specific *Pten*-deficient mice by crossing $Pten^{fl/fl}$ mice with $Il17a^{cre}$ mice to generate $Pten^{fl/fl}Il17a^{cre}$ mice. We then confirmed that deletion of *Pten* occurs in a Th17-specific manner (Fig. 1 C) and mostly within 12 h after TCR stimulation (Fig. 1 D) in cells from $Pten^{fl/fl}Il17a^{cre}$ mice. T cell and B cell development (Fig. S1 A), $CD4^+$ and $CD8^+$ T cell development (Fig. S1 B), and naive and effector $CD4^+$ T cell development (Fig. S1 C) in various lymphoid tissues of $Pten^{fl/fl}Il17a^{cre}$ mice were comparable with those of control mice. To investigate whether *Pten* deficiency inhibits Th17 cell differentiation, we stimulated naive $CD4^+$ T cells from two different control (either $Pten^{fl/fl}$ or $Il17a^{cre}$) or $Pten^{fl/fl}Il17a^{cre}$ mice under Th1-, Th2-, Th17-, and T reg–polarizing conditions and examined expression of signature genes within each subset. Surprisingly, expression of IL-17A was completely abolished and that of *Rorc* and *Il23r* was greatly reduced in *Pten*-deficient Th17 cells (Fig. 1, E and F; and Fig. S2, A and B). Expression of Th1/Th2-related genes such as *Ifng*, *Il4*, *Tbx21*, and *Gata3* was not changed by *Pten* deletion (Fig. 1 F). However, expression of *Foxp3*, *Il10*, *Tgfb1*, and *Gzmb* increased upon *Pten* deletion (Fig. 1 F). These results suggest that PTEN affects mainly Th17- and T reg–related genes and that the increase of T reg–related genes might be a result of diminished Th17 cell differentiation.

Because the *Pten* gene is deleted after IL-17 expression in the $Pten^{fl/fl}Il17a^{cre}$ mice, these results suggest the importance of PTEN in already committed Th17 cells. To examine the effect of PTEN on Th17 cell differentiation from naive CD4 T cells, we next examined the effect of PTEN knockdown on Th17 cell differentiation in vitro. Three candidate shRNAs targeting PTEN were generated using the MSCV-LMP vector, and reduced expression of PTEN protein was confirmed (Fig. 1 G). Transduction of retroviral *Pten*-shRNA into Th17 cells reduced the levels of *Il17a* mRNA (Fig. 1 H) and the $IL\text{-}17A^+$ cell population (Fig. 1 I). Collectively, these data indicate that PTEN is required for Th17 cell differentiation in vitro.

Pten deficiency ameliorates Th17-mediated inflammation

Next, we asked whether Th17-specific *Pten* deficiency inhibits Th17-induced inflammation in vivo. To this end, we used an EAE model, which is a model representative of human disease induced by Th17 cells (Cua et al., 2003; Komiyama et al., 2006). We first injected control $Pten^{fl/fl}$ and $Pten^{fl/fl}Il17a^{cre}$ mice with a myelin oligodendrocyte glycoprotein ($MOG_{35–55}$) peptide (emulsified in CFA) and pertussis toxin to induce EAE. Clinical scores (based on observed symptoms; see Materials and methods) were then measured. $Pten^{fl/fl}Il17a^{cre}$ mice were resistant to EAE induction, whereas $Pten^{fl/fl}$ mice showed symptoms (Fig. 2 A). Mice were sacrificed on day 20, and spinal cords were harvested and examined by staining with hematoxylin and eosin (H&E) and Luxol fast blue (Fig. 2, B and C). Spinal cords from $Pten^{fl/fl}$ mice showed severe inflammation (Fig. 2 B) and demyelination (Fig. 2 C). In contrast, those from $Pten^{fl/fl}Il17a^{cre}$ mice showed less severe inflammation (Fig. 2 B) and demyelination (Fig. 2 C). We next harvested the central nervous system (CNS) from EAE-induced $Pten^{fl/fl}$ and $Pten^{fl/fl}Il17a^{cre}$ mice and analyzed infiltrating cells by flow cytometry. The percentage and number of $IL\text{-}17A^+$ cells and $GM\text{-}CSF^+$ cells in the CNS of $Pten^{fl/fl}Il17a^{cre}$ mice were markedly lower than those in $Pten^{fl/fl}$ mice (Fig. 2, D–F). In contrast, the percentage and number of T reg cells in the CNS of $Pten^{fl/fl}Il17a^{cre}$ mice were markedly higher than those of $Pten^{fl/fl}$ mice (Fig. 2, D and G). The percentage and number of total $CD4^+$ cells in the CNS of $Pten^{fl/fl}Il17a^{cre}$ mice were also lower (Fig. 2 H). Of note, the number of $CD4^+$ $IFN\text{-}\gamma^+$ cells in the CNS of $Pten^{fl/fl}Il17a^{cre}$ mice was slightly lower than that in $Pten^{fl/fl}$ mice, although the percentage remained unchanged (Fig. 2 I). Previous studies show that ex-Th17 cells produce proinflammatory cytokines, including IFN-γ, during EAE development (Lee et al., 2009; O'Shea and Paul, 2010; Hirota et al., 2011). Thus, the reduced number of $CD4^+IFN\text{-}\gamma^+$ cells could be a result of a reduction in the number of IL-17A–producing cells. Next, we examined the amount of mRNA encoding various signature genes expressed by CNS-infiltrating mononuclear cells (Fig. 2 J). Expression of Th17 signature genes, including *Il17a*, *Il23r*, and *Rorc*, but not *Ifng* and *Foxp3*, was markedly reduced in cells from $Pten^{fl/fl}Il17a^{cre}$ mice (Fig. 2 J). Collectively, these results indicate that Th17-specific *Pten* deletion inhibits Th17 cell differentiation and effector function in an EAE model.

Because neutrophils and γ:δ T cells also express IL-17A, we examined whether they are also defective in *Pten* expression in $MOG_{35–55}$ peptide-injected mice. We found that *Pten* expression was lower in neutrophils, γ:δ T cells, and ILC3 cells isolated from the spleen, peripheral blood, and intestine of $Pten^{fl/fl}Il17a^{cre}$ mice than in those isolated from control mice; this was not the case for dendritic cells, which do not produce IL-17A (Fig. 3 A). However, the percentage of γ:δ T cells in the spleen, peripheral LNs (pLNs), and thymus was

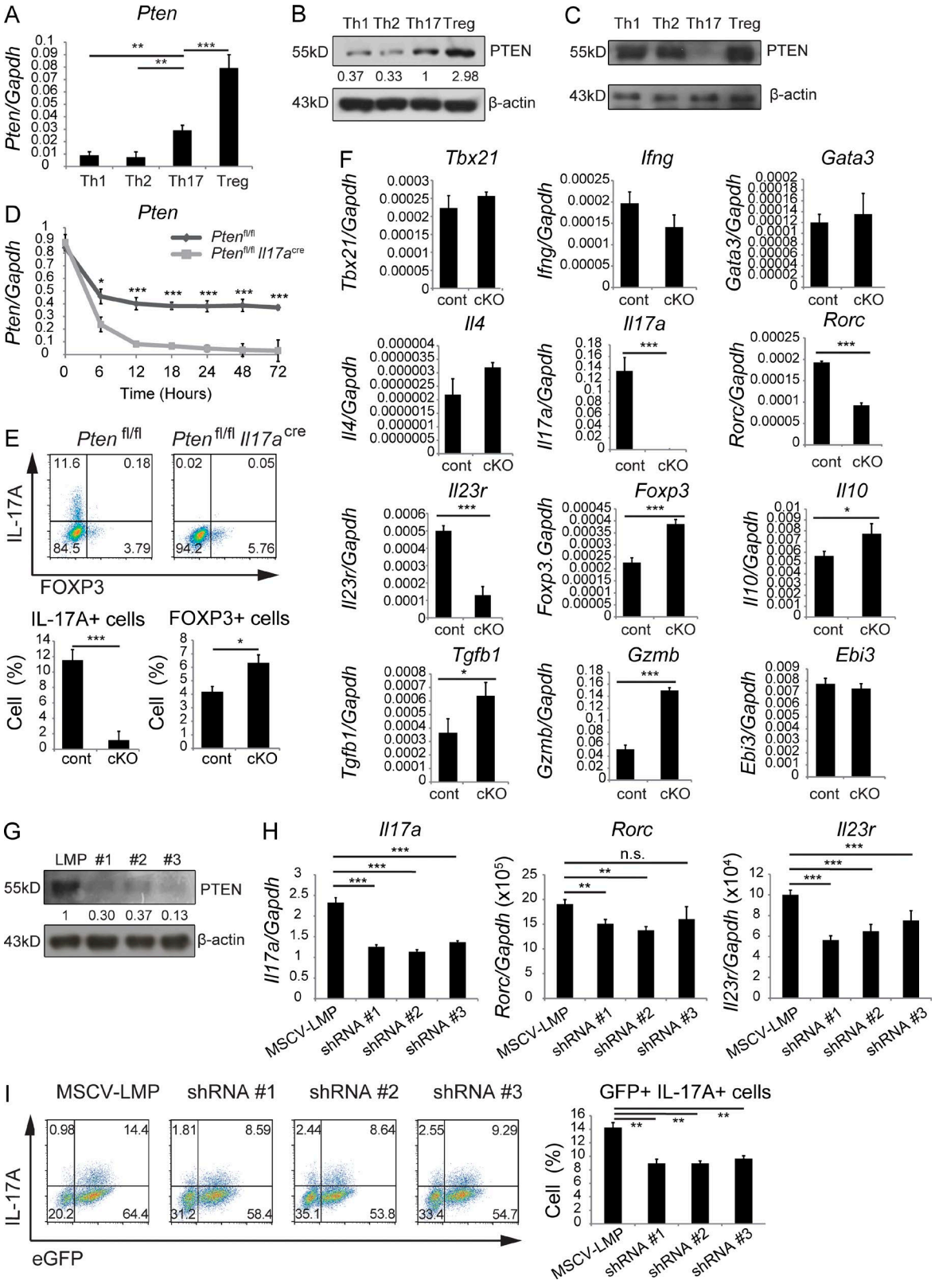

Figure 1. **Th17 cell–specific *Pten* deficiency or knockdown inhibits Th17 cell differentiation in vitro.** (A and B) PTEN expression. Naive CD4$^+$ T cells were stimulated under polarizing conditions for 3 d to enable differentiation into different subsets. (A) Level of *Pten* mRNA in each subset was measured by qRT-PCR. (B) Whole cell lysates were then run on SDS-PAGE gels, and PTEN protein levels were measured by immunoblotting and quantitated by

not altered by deletion of *Pten* (Fig. 3 B). To further examine alterations in the IL-17A producing capacity of γ:δ T cells from *Pten*$^{fl/fl}$*Il17a*^{cre} mice, we isolated splenocytes from WT and *Pten*$^{fl/fl}$*Il17a*^{cre} mice, stimulated them with PMA and ionomycin for 4 h, and analyzed IL-17A–producing cells by flow cytometry. The percentage of IL-17A–producing CD4 T cells decreased, but that of IL-17A–producing γ:δ T cells did not, upon IL-17A–specific deletion of *Pten* (Fig. 3 C), suggesting that γ:δ T cells are not major players in the diminished IL-17A–mediated inflammation observed in *Pten*$^{fl/fl}$*Il17a*^{cre} mice. During steady-state, a significant fraction of intestinal CD4 T cells are Th17 cells, the presence of which impacts EAE severity (Lee et al., 2011). Indeed, *Pten*$^{fl/fl}$*Il17a*^{cre} mice had fewer Th17 cells in the colonic lamina propria (Fig. 3 D), suggesting a possible role for these cells.

Pten deficiency promotes IL-2 expression by Th17 cells

Next, we explored the molecular mechanism underlying PTEN-mediated Th17 cell differentiation. PTEN acts as a negative regulator of PI3K signaling by dephosphorylating PIP_3 to yield PIP_2, thereby reversing PI3K signaling (Stambolic et al., 1998). PI3K/Akt signaling acts downstream of signals transduced by the TCR or CD28 (Ward et al., 1992). Previous studies reveal that the PI3K/Akt signaling cascade induces IL-2 expression in T cells and regulates their proliferation and survival (Eder et al., 1998; Kane et al., 1999, 2001). Previous studies also show that IL-2 inhibits Th17 cell differentiation (Laurence et al., 2007; Liao et al., 2011; Yang et al., 2011). Thus, we hypothesized that *Pten* deficiency induces IL-2 production in Th17 cells, and that increased IL-2 levels eventually block Th17 cell differentiation. To test this, we first examined IL-2 expression in *Pten*-deficient Th17 cells. We stimulated naive CD4 T cells from *Pten*$^{fl/fl}$ and *Pten*$^{fl/fl}$ *Il17a*^{cre} mice under Th17-polarizing conditions by TGF-β, IL-6, IL-1β, and TNF for 3 d and then measured the amount of *Il*2 mRNA on a daily basis (Fig. 4). The amount of *Il2* mRNA in *Pten*-deficient cells on day 1 (Fig. 4 A, left) and day 2 (Fig. 4 A, right) was significantly higher than that in the control group. Next, we examined expression of IL-2 protein in Th17 cells (Fig. 4 B) and in the culture medium (Fig. 4 C). *Pten* deficiency greatly induced expression of IL-2 protein by Th17 cells (Fig. 4, B and C). To examine the possibility that PTEN is important for Th17 cell differentiation in the presence of only certain combinations of cytokines (e.g., TGF-β/IL-6/IL-1β/TNF used in the aforementioned experiment), we examined PTEN-mediated regulation of IL-2 in the presence of a different combination of polarizing cytokines. When we used a cytokine combination of IL-1β/IL-6/IL-23, we observed induction of IL-2 and a reduction of IL-17 (similar to the combination of TGF-β/IL-6/IL-1β/TNF; Fig. S2 C), excluding the possibility that only certain cytokine combinations are relevant. We next used a transient reporter assay and a siRNA-mediated knockdown approach to confirm that *Pten* deficiency promotes IL-2 expression. We first transfected an EL4 cell line with a pGL3-*Il2* promoter vector and control siRNA or PTEN siRNA and then measured *Il2* promoter activity using a dual luciferase assay (Fig. 4 D). PTEN knockdown induced *Il2* promoter activity in a PTEN siRNA dose-dependent manner. IL-17A production by *Pten*-deficient cells was restored when a neutralizing anti–IL-2 antibody was added to the culture medium (Fig. 4, E and F), suggesting that IL-2 is a critical mediator of *Pten* deficiency. Collectively, these results indicate that *Pten* deficiency induces IL-2 expression in Th17 cells, and that increased IL-2 expression inhibits Th17 cell differentiation.

Pten deficiency activates STAT5 in Th17 cells

Next, we examined whether *Pten* deficiency induces phosphorylation of components downstream of the PI3K/Akt signaling pathway. We examined Akt phosphorylation at S473 and T308, which are well-known phosphorylation sites on the Akt molecule (Fig. 5, A and B; Fresno Vara et al., 2004). We found that *Pten* deficiency promoted phosphorylation at both sites. However, phosphorylation of S6, which is downstream of the mTORC1 signal cascade, was no different in WT and *Pten*-deficient cells (Fig. 5 C), suggesting that PTEN does not affect mTORC1 signaling.

Previous studies show that IL-2 inhibits expression of Th17 signature genes by simultaneously activating STAT5 phosphorylation and inactivating STAT3 phosphorylation (Laurence et al., 2007; Yang et al., 2011). Because IL-2 production increased in *Pten*-deficient Th17 cells, we next examined phosphorylation of STAT5 and STAT3 in *Pten*-deficient Th17 cells (Fig. 5, D and E). As predicted, STAT5 phosphor-

densitometry. β-Actin was used as a loading control (cont). (C–F) *Pten* deficiency. (C) Naive CD4$^+$ T cells were stimulated as in (A), and PTEN protein levels were measured by immunoblotting. (D) Expression of *Pten* mRNA in Th17 was measured in a time-dependent manner. Naive CD4$^+$ T cells from WT (*Pten*$^{fl/fl}$) and cKO (*Pten*$^{fl/fl}$*Il17a*^{cre}) mice were cultured under Th17-polarizing conditions and harvested at the indicated time points. (E) IL-17A$^+$ and FOXP3$^+$ cells were measured by flow cytometry. Naive CD4$^+$ T cells from WT (*Pten*$^{fl/fl}$) and cKO (*Pten*$^{fl/fl}$*Il17a*^{cre}) mice were cultured under Th17-polarizing conditions for 3 d. Data were pooled from three individual experiments (bottom). (F) Levels of *Ifnγ* mRNA in Th1, *Il4* mRNA in Th2, *Il17a, Rorc,* and *Il23r* mRNA in Th17, and *Foxp3* mRNA in T reg cells were measured by qRT-PCR. Expression of *Il10*, *Tgfb1*, *Gzmb*, and *Ebi3* mRNA in Th17 cells was measured by qRT-PCR. (G–I) PTEN knockdown. (G) Naive CD4$^+$ T cells were transfected with control (LMP) or *Pten*-shRNAs (#1, #2, and #3). Transfected cells were then harvested, and whole cell lysates were run on SDS-PAGE gels. PTEN protein levels were measured by immunoblotting and quantitated by densitometry. (H and I) *Il17a, Rorc*, and *Il23r* mRNA levels by qRT-PCR (H). Data were normalized to *Gapdh* expression. IL-17A cytokine levels in transfected cells were measured by flow cytometry (I). Data were pooled from three individual experiments (right). Data in A, D, F, and H were pooled from three individual experiments, and data in E and I represent three independent experiments. Error bars represent the SD. Statistical differences between groups were determined by the Student *t* test. *, $P < 0.05$; **, $P < 0.01$; and ***, $P < 0.001$. n.s., not significant.

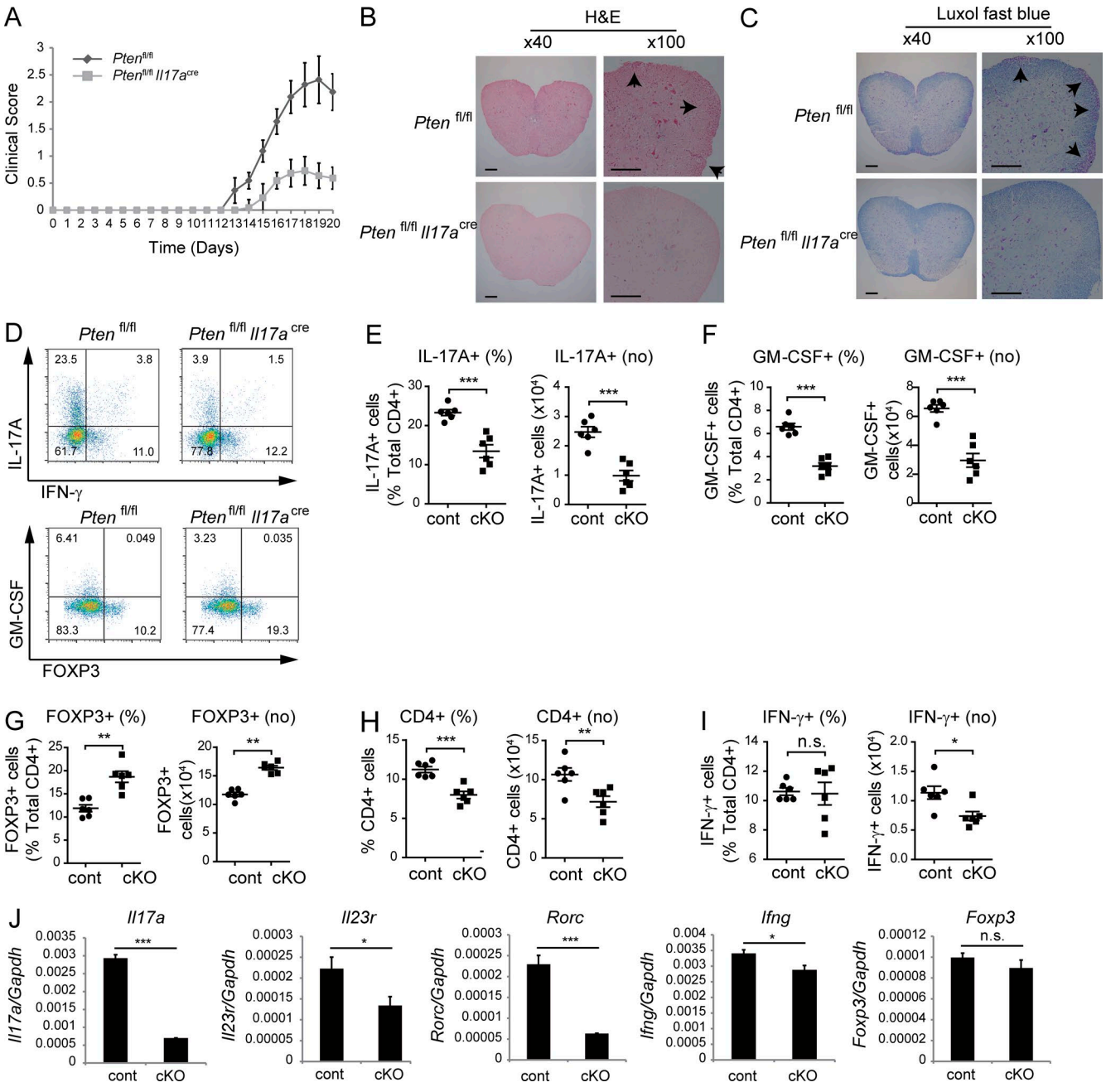

Figure 2. **Th17-specific *Pten* deficiency ameliorates neuroinflammation in EAE mice.** (A) Clinical scores for WT (*Pten*$^{fl/fl}$) and cKO (*Pten*$^{fl/fl}$*Il17a*^{cre}) mice (n = 11) after EAE induction. (B and C) Histopathological analysis of lumbar spinal cords from WT and cKO mice at the peak of the disease. (B) H&E-stained sections of spinal cords from WT and cKO mice. Arrows highlight inflammatory foci. Bars, 100 µm. (C) Luxol fast blue–stained sections of spinal cords from WT and cKO mice. Arrows highlight demyelinated foci. Bars, 100 µm. (D) IFN-γ and IL-17A expression (top) and GM-CSF and FOXP3 expression (bottom) by CD4$^+$ cells from the CNS were measured by flow cytometry. (E–I) The percentage and absolute number (no) of cells infiltrating the CNS were measured. (E) IL-17A$^+$ cells, (F) GM-CSF$^+$ cells, (G) FOXP3$^+$ cells, (H) CD4$^+$ cells, and (I) IFN-γ$^+$ cells. (J) The amount of *Il17a*, *Il23r*, *Rorc*, *ifng*, and *Foxp3* mRNA in mononuclear cells isolated from the CNS was measured by qRT-PCR. Data were normalized to *Gapdh* expression. Data in D are representative of six independent experiments, and data in E–J are pooled from six independent experiments. Error bars represent the SD. Statistical differences between groups were determined by the Student *t* test. *, P < 0.05; **, P < 0.01; and ***, P < 0.001. n.s., not significant.

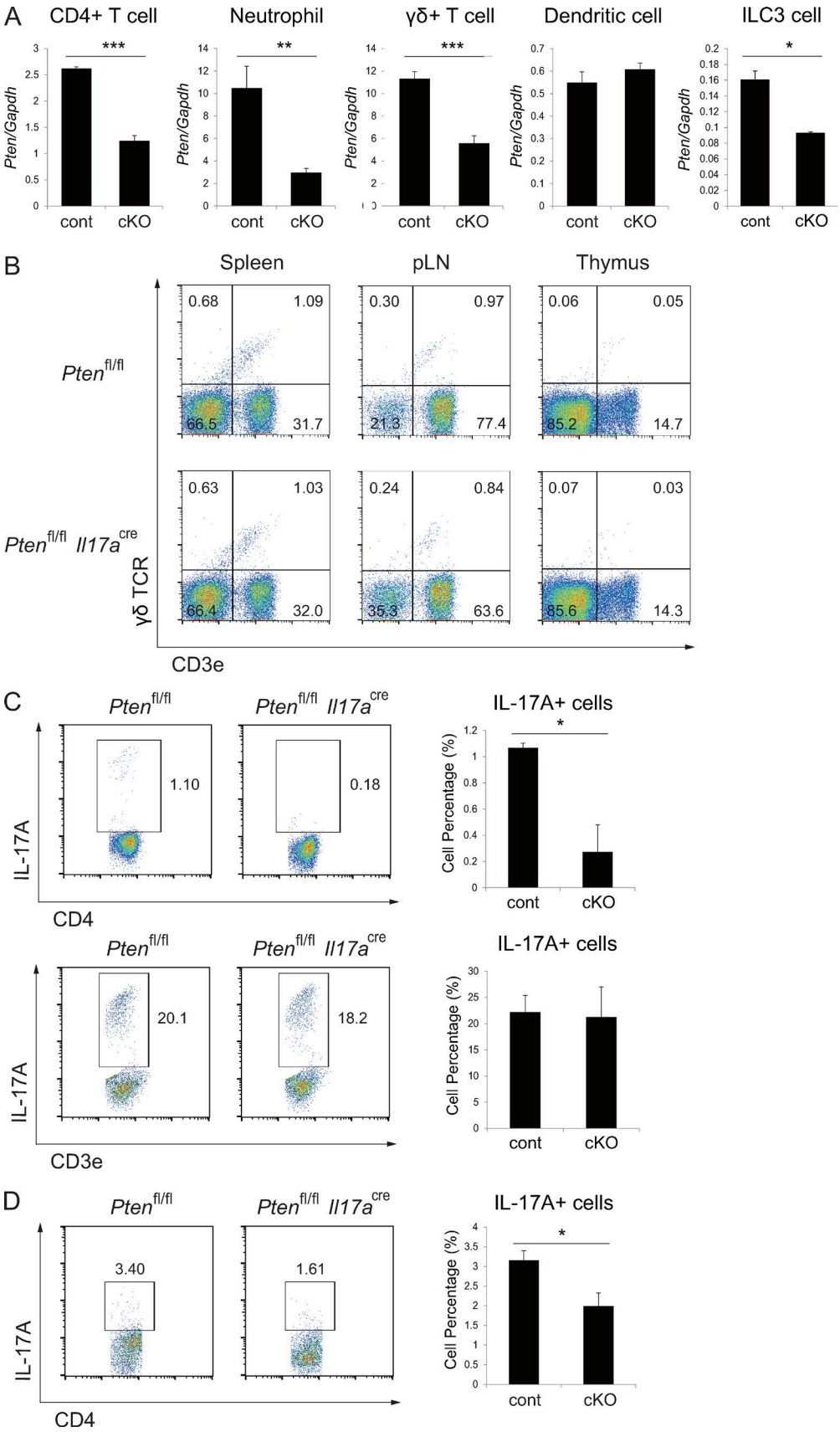
A
CD4+ T cell
Neutrophil
γδ+ T cell
Dendritic cell
ILC3 cell
Pten/Gapdh
cont
cKO
B
Spleen
pLN
Thymus
Ptenfl/fl
Ptenfl/fl Il17acre
γδ TCR
CD3e
C
Ptenfl/fl
Ptenfl/fl Il17acre
IL-17A
CD4
IL-17A+ cells
Cell Percentage (%)
D
CD3e

ylation increased but STAT3 decreased compared with WT Th17 cells, indicating that *Pten* deficiency induces changes in the phosphorylation status of STAT5 and STAT3, which inhibit Th17 cell differentiation. Expression of IL-6R was also reduced in *Pten*-deficient Th17 cells (Fig. 5 F), suggesting that it may be related to reduction of STAT3 phosphorylation. Moreover, when a STAT5 inhibitor was added to *Pten*-deficient Th17 cells, IL-17A expression was restored (Fig. 5, G and H). Collectively, these results demonstrate that *Pten* deficiency activates STAT5 and IL-2 signaling, which in turn inhibits Th17 cell differentiation.

Pten deficiency causes alteration of gene expression profile in Th17 cells

To examine whether *Pten* deficiency alters global gene expression profiles, we performed microarray analysis with in vitro–differentiated Th17 cells from WT and $Pten^{fl/fl}Il17a^{cre}$ mice (Dataset S1 and GEO accession no. GSE102414). Gene ontology analysis revealed that the top three gene categories altered in *Pten*-deficient Th17 cells were immune response, regulation of cell proliferation, and defense response (Fig. 6 A). The expression of genes related to Th17 cell differentiation and function decreased, whereas that related to T reg cell differentiation and function increased, in *Pten*-deficient Th17 cells (Fig. 6 B), which is consistent with the aforementioned results. We also analyzed expression of transcription factors that regulate *Il2* transcription (Kim et al., 2006) in *Pten*-deficient Th17 cells. Among them, expression of *Crem* and *Satb1*, which are negative regulators (Tenbrock et al., 2002, 2003; Kumar et al., 2005), decreased, but that of *Egr1*, a positive regulator (Decker et al., 1998), increased (Fig. 6 C), providing a clue to the molecular mechanism underlying increased IL-2 expression in these cells.

PTEN inhibitors block Th17 cell differentiation in vitro

Because the aforementioned results suggest that PTEN is a critical regulator of Th17 cell differentiation and Th17-mediated disease, we next examined the possibility that inhibitors of PTEN can prevent or treat Th17-mediated disease.

As a first step, we asked whether inhibitors of PTEN inhibit Th17 cell differentiation in vitro. First, we used SF1670, the most potent PTEN-specific inhibitor (Li et al., 2011). Naive $CD4^+$ T cells were cultured under Th0-polarizing conditions in the presence of SF1670, and the amount of *Il17a* and *Foxp3* mRNA was measured by quantitative RT-PCR (qRT-PCR). SF1670 treatment led to a marked reduction in the amount of *Il7a* mRNA but to a slight increase in the amount of *Foxp3* mRNA (Fig. 7 A). Next, we cultured naive $CD4^+$ T cells under Th17-polarizing conditions in the presence of SF1670 and measured expression of IL-17A and FOXP3 protein (Fig. 7, B and C) and of *Il17a* and *Rorc* mRNA (Fig. 7 D). Consistent with the gene-deficiency experiments, SF1670 led to a marked reduction in expression of Th17 signature genes in a dose-dependent manner (Fig. 7 D). Furthermore, SF1670 induced FOXP3 expression under induced T reg conditions (Fig. S3). These data indicate that SF1670 controls the Th17/T reg balance by regulating IL-17A/FOXP3 expression. To confirm this, we repeated the experiments with another PTEN inhibitor, bpv(phen) (Schmid et al., 2004). Bpv(phen) also reduced expression of Th17-related genes but induced expression of FOXP3 under Th17-polarizing conditions in a dose-dependent manner (Fig. S4). We then used 7AAD and Annexin V double staining to examine cell viability in the presence of a PTEN inhibitor (Fig. 7 E and Fig. S4 D) and in an MTS assay (Fig. 7 F and Fig. S4 E). Cell viability, as measured by both methods, was unaffected by the PTEN inhibitors. These results indicate that PTEN inhibitors interrupt Th17 cell differentiation in vitro.

Inhibition of PTEN ameliorates EAE symptoms

Finally, we examined the therapeutic effects of SF1670 in EAE mice. EAE was induced by injecting mice with a $MOG_{35–55}$ peptide (emulsified in CFA) and pertussis toxin on day 0, followed by an additional injection of pertussis toxin on day 2. The mice were then injected with SF1670 (1 μmol/kg) every other day from day 2 and sacrificed at day 20 (Fig. 8 A). SF1670 effectively ameliorated the symptoms of EAE (Fig. 8 B). The percentage and number of CNS-infiltrating $IL\text{-}17A^+$ cells was lower in SF1670-treated mice than in untreated mice (Fig. 8, C and D), whereas the percentage and number of CD4, IFN-γ^+, IL-17^+IFN-γ^+, CD8 cells, and granulocytes was unchanged (Fig. 8, E–G; and Fig. S5, A and B). Cell number of macrophages was slightly decreased by SF1670, but the percentage was not changed (Fig. S5, A and B). In addition, the percentage of infiltrating $FOXP3^+$ T reg cells was slightly higher after SF1670 treatment (Fig. 8 H, left); however, the absolute number of cells was unchanged (Fig. 8 H, right). Moreover, the amount of *Il17a* and *Rorc* mRNA in CNS-infiltrated mononuclear cells was greatly reduced, whereas that of Foxp3 increased

Figure 3. **γ:δ T cells are not altered in *Pten* cKO mice.** (A) *Pten* mRNA expression in $CD4^+$ T cells, neutrophils, γ:δ T cells, dendritic cells, and ILC3 cells was measured by qRT-PCR. Each cell type was isolated from WT ($Pten^{fl/fl}$) and cKO ($Pten^{fl/fl}Il17a^{cre}$) mice. Data were normalized to *Gapdh* expression. Data were pooled from three individual experiments. (B) Development of γ:δ T cells in the spleen, pLNs, and thymus was measured by flow cytometry after cells were isolated from WT and cKO mice. (C) Splenocytes from WT and cKO mice were stimulated with PMA/ionomycin for 4 h, and gated on $CD3\varepsilon^+$ $CD4^+$ population (top) or $CD3\varepsilon^+$ γ:δ TCR^+ population (bottom), and IL-17A expression was measured. Data were pooled from three individual experiments (right). (D) Mononuclear cells were isolated from colonic lamina propria. Cells were stimulated with PMA/ionomycin for 4 h, and IL-17A expression by $CD4^+$ T cells was measured by flow cytometry. Data were pooled from three individual experiments (right). Dot plot data in B–D are representative of three individual experiments. Error bars represent the SD. Statistical differences between groups were determined by the Student *t* test. *, $P < 0.05$; **, $P < 0.01$; and ***, $P < 0.001$.

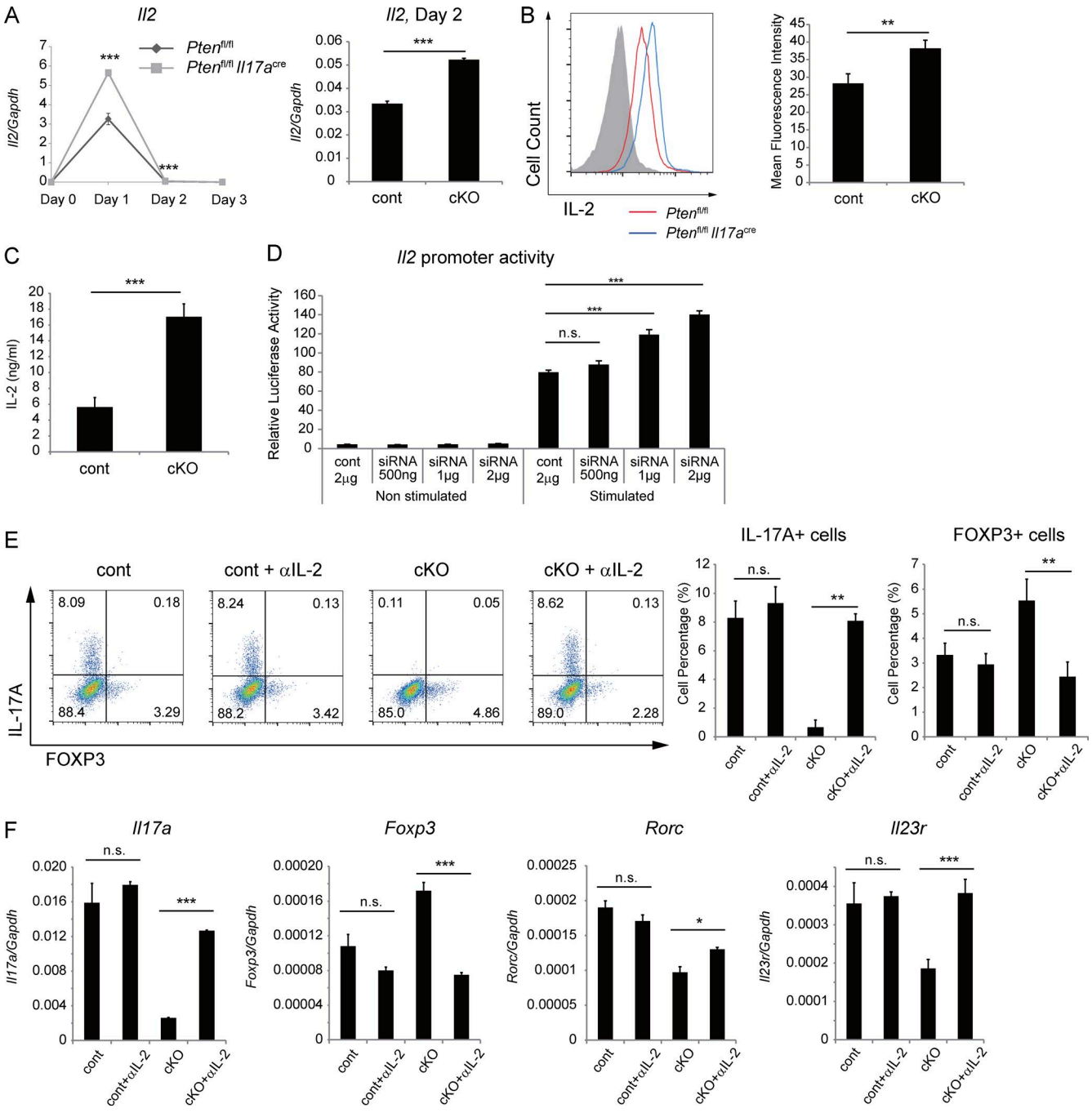

Figure 4. ***Pten* deficiency promotes IL-2 production in Th17 cells.** (A) *Il2* mRNA levels at days 1, 2, and 3 of culture were measured by qRT-PCR (left). *Il2* mRNA levels at day 2 are presented separately (right). Naive CD4$^+$ T cells from WT (*Pten*$^{fl/fl}$; black line) and cKO (*Pten*$^{fl/fl}$*Il17a*^{cre}; gray line) mice were cultured under Th17-polarizing conditions. Data were normalized to *Gapdh* expression. (B and C) IL-2 was measured by flow cytometry (B). Cells from WT (red line) and cKO (blue line) mice were cultured under Th17-polarizing conditions for 3 d. (C) IL-2 cytokine levels in the supernatant of cultured cells were measured by ELISA. Cells were cultured under the same conditions as in (B). (D) *Il2* promoter activity was measured in a dual luciferase assay. EL4 cells were transfected with varying concentrations of the pGL3-*il2* promoter vector and PTEN siRNA. Relative luciferase activity was calculated by dividing *Firefly* luciferase activity by *Renilla* luciferase activity. Cont, control siRNA. (E and F) IL-17A and FOXP3 expression was measured by flow cytometry (E), and *Il17a*, *Rorc*, *Il23r*, and *Foxp3* mRNA levels were measured by qRT-PCR (F). Data were pooled from three individual experiments (E, right). Naive CD4$^+$ T cells from WT and cKO mice were cultured under Th17-polarizing conditions in the presence of an anti–IL-2 antibody (S4B6). Dot plot data represent three independent experiments, and data in A–D and F were pooled from three independent experiments. Error bars represent the SD. Statistical differences between groups were determined by the Student *t* test. *, $P < 0.05$; **, $P < 0.01$; and ***, $P < 0.001$. n.s., not significant.

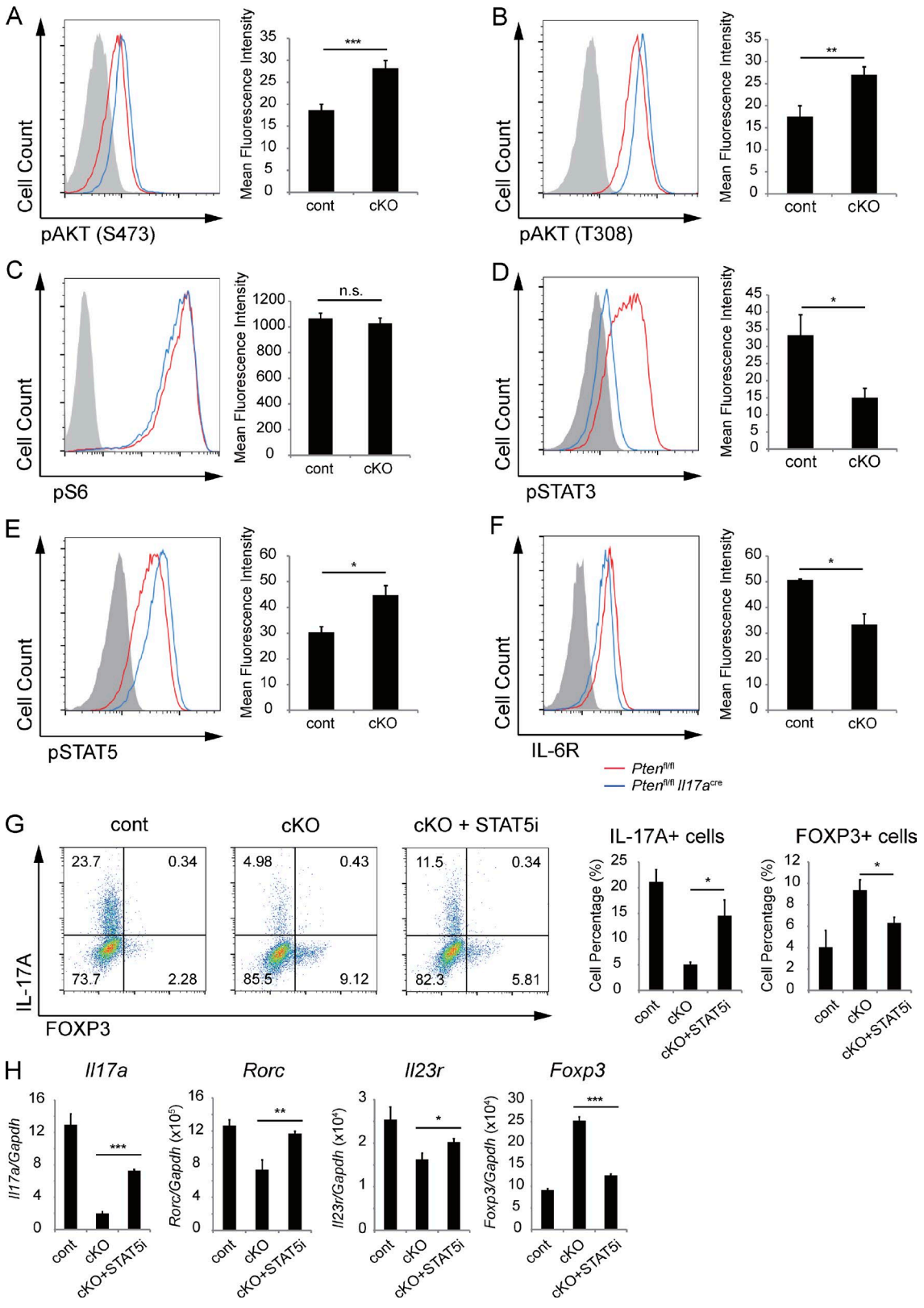

Figure 5. ***Pten* deficiency in Th17 cells induces phosphorylation of STAT5.** (A–F) pAkt (S473) (A), pAkt (T308) (B), pS6 (C), pSTAT3 (D), pSTAT5 (E), and IL-6R (F) expression was measured by flow cytometry. Mean fluorescence intensity of each experiment was measured and pooled from three independent experiments (right). Naive CD4$^+$ T cells from WT (*Pten*$^{fl/fl}$; red line) and cKO (*Pten*$^{fl/fl}$*Il17a*^{cre}; blue line) mice were cultured under Th17-polarizing conditions

(Fig. 8 I). Because deleting PTEN from APCs modulates EAE severity (Blüml et al., 2015; Sahin et al., 2015), the aforementioned results may be caused by pharmacologic inhibition of Th17 cells, APCs, or both. We addressed this question by treating EAE-induced *Pten*$^{fl/fl}$*Il17a*^{cre} mice with an inhibitor, SF1670. We then measured the effect of the PTEN inhibitor on non–IL-17 producer cells. SF1670 did not cause further decrease in EAE severity (Fig. S5 C), suggesting that the inhibitor mainly affects IL-17$^+$ cells. Collectively, these results demonstrate that PTEN inhibitor SF1670 effectively blocks Th17-mediated inflammation in vivo.

DISCUSSION

Here, we show that PTEN plays an important role in Th17 cell differentiation. To explore the Th17-intrinsic role of PTEN, we first generated *Pten*$^{fl/fl}$*Il17a*^{cre} mice, which harbor Th17 cells lacking *Pten*. We then used an EAE model to show that Th17-specific *Pten* deletion ameliorates the symptoms of EAE by inhibiting Th17 cell differentiation. *Pten* deficiency increased IL-2 expression, which signals through STAT5 to inhibit Th17 cell differentiation. Furthermore, a PTEN inhibitor, SF1670, efficiently blocked Th17 cell differentiation in vitro and ameliorated EAE symptoms. These results indicate that PTEN is an important regulator of Th17 cell differentiation, and that inhibiting PTEN may be a potential therapeutic strategy for Th17-mediated autoimmune diseases.

Th17 cells have features distinct from those of other CD4$^+$ effector T cells. One such feature is that they show different responses to CD28 costimulatory signals. CD28 costimulatory signaling promotes homeostatic proliferation and activation of CD4$^+$ T cells by inducing IL-2 expression (June et al., 1987; Boyman and Sprent, 2012). However, CD28 signaling is not helpful for Th17 cell differentiation because it inhibits Th17 cell development and blocks IL-17A cytokine expression (Bouguermouh et al., 2009). Furthermore, recent studies reveal that IL-2 inhibits Th17 cell differentiation directly by silencing the *Il17a* gene independently of crucial transcription factors such as FOXP3 and RORγt (Elias et al., 2008). This differential reactivity to IL-2 can be used to selectively inhibit Th17 cell differentiation and function and, thus, cure Th17-mediated diseases. The present study describes one example of this by demonstrating that PTEN inhibition induces IL-2 production, thereby selectively inhibiting Th17 cell differentiation and ameliorating EAE.

The role of the PI3K pathway in Th17 cell differentiation is controversial. Kurebayashi et al. (2012) used PI3K p85α-deficient mice or a selective inhibitor of PI3K p110δ and found that blocking the PI3K/Akt/mTOR pathway inhibits Th17 cell differentiation because of a failure to repress Gfi1 expression and a failure to translocate RORγ. However, Pierau et al. (2009) used constitutively active Akt transgenic mice to show that increased PI3K/Akt signaling also impairs Th17 cell differentiation. The reason for these different results is not clear at this time. One possible explanation for the discrepancy is the different experimental systems used; one is a loss-of-function system whereas the other is a gain-of-function system. Another possible explanation is that regulation of PI3K/Akt signaling may require a narrow window of activity as it seems that either inhibiting or overactivating the PI3K/Akt signaling pathway inhibits Th17 cell differentiation. This delicate balance is manifested by well-known *Pten* haploinsufficiency phenotypes in the immune system (Di Cristofano et al., 1999). *Pten* heterozygote mice develop a progressive lymphoproliferative, autoimmune phenotype that becomes clinically overt by 6–9 mo of age (Di Cristofano et al., 1999). Further experiments are needed to resolve these discrepancies.

Some studies reported that PTEN down-regulates STAT3 activation by dephosphorylating Y705 in human papillomavirus-infected cells (Sun and Steinberg, 2002) and that PTEN inhibits phosphorylation of Akt and STAT3 in a glioblastoma cell line (Moon et al., 2013). On the other hand, PTEN-deficiency triggers the signaling cascades that inhibit STAT3 activation in mouse astrocytes and human glioblastoma tumors (de la Iglesia et al., 2008a,b). Our current study shows that PTEN-deficiency caused inhibition of STAT3 in CD4 T cells. Thus, it seems that whether PTEN activates or inhibits STAT3 depends on cellular context. The role of PTEN in autoimmunity also seems to be context-dependent. It has been reported that PTEN overexpression ameliorates autoimmune arthritis through down-regulating STAT3 activation (Lee et al., 2016). In contrast, it has been also reported that loss of PTEN in myeloid cells decreases autoimmune arthritis progression in a mouse model (Blüml et al., 2015; Sahin et al., 2015). These studies suggest that the role of PTEN is context-dependent and that different methods of experiments, overexpression versus deletion, could yield different results. As we discussed above that regulation of PI3K/Akt signaling may require a narrow window of activity in Th17 cell differentiation, the amount of PTEN may have a critical range to exert certain physiological effect.

Previously, Akt signaling was considered to play a crucial role in autoimmunity, and PTEN was believed to regulate autoimmunity (Ward et al., 1992; Soond et al., 2012). Indeed,

for 3 d. (G) Naive CD4$^+$ T cells from WT (*Pten*$^{fl/fl}$) and cKO (*Pten*$^{fl/fl}$*Il17a*^{cre}) mice were cultured under Th17-polarizing conditions for 3 d in the presence or absence of a STAT5 inhibitor (10 µM). The percentage and number of IL-17A$^+$ and FOXP3$^+$ cells were measured by flow cytometry. Data were pooled from three individual experiments (right). (H) Cells were cultured under the same conditions described in (G). *Il17a, Rorc, Il23r,* and *Foxp3* mRNA levels were measured by qRT-PCR, and data were normalized to *Gapdh* expression. Data were pooled from three independent experiments. Flow cytometry data represent three independent experiments. Error bars represent the SD. Statistical differences between groups were determined by the Student *t* test. *, $P < 0.05$; **, $P < 0.01$; and ***, $P < 0.001$. n.s., not significant.

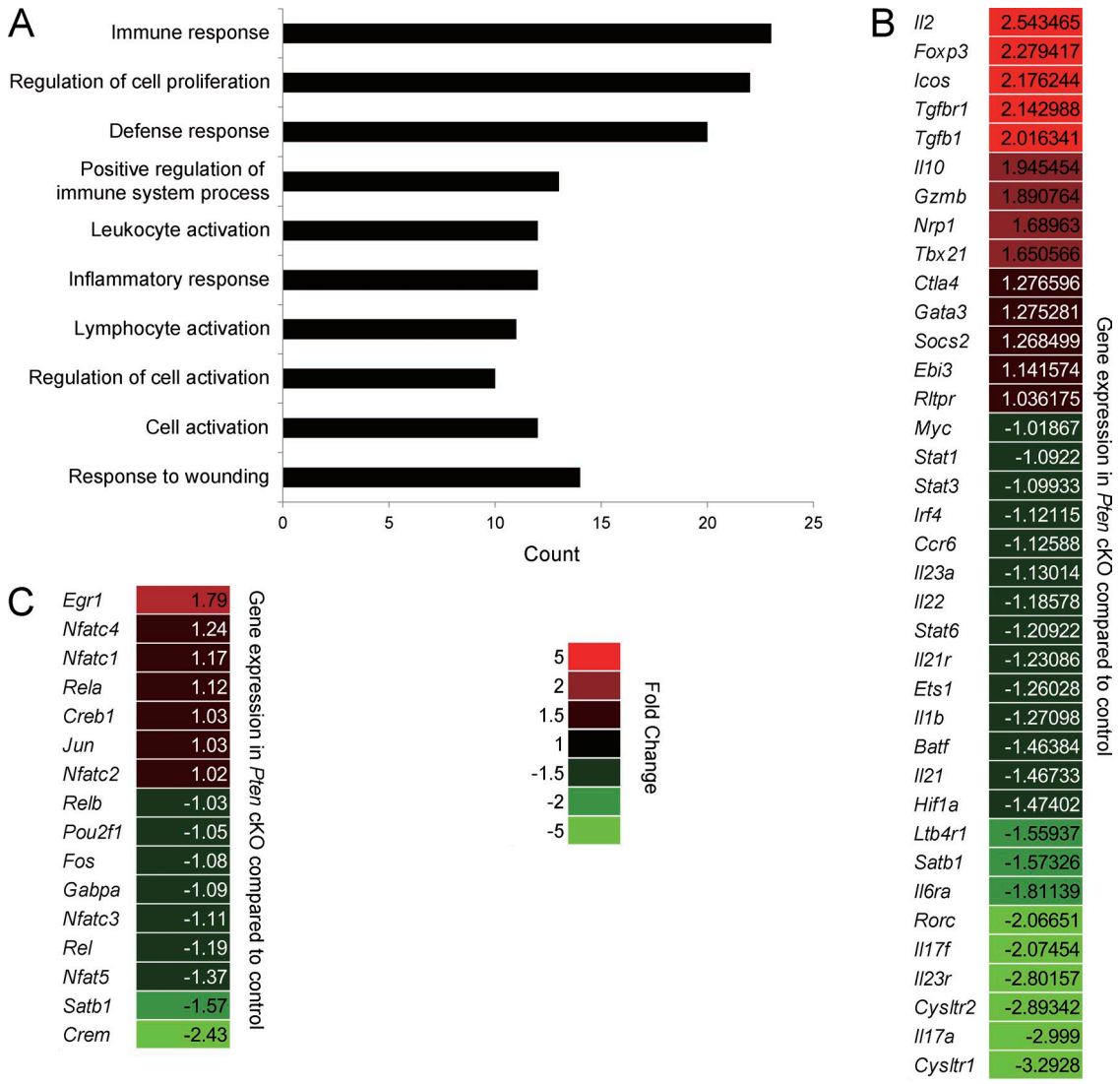

Figure 6. ***Pten* deficiency causes an alteration of gene expression profile in Th17 cells.** (A) Gene ontology analysis of genes differentially expressed in Th17 cells from WT (*Pten*$^{fl/fl}$) and *Pten* cKO (*Pten*$^{fl/fl}$*Il17a*^{cre}) mice. (B) Heat map of representative signature genes of Th17 and T reg cells expressed in WT and *Pten* cKO Th17 cells. (C) Heat map of representative genes associated with *Il2* expression in WT and *Pten* cKO Th17 cells.

some studies report that *Pten* deficiency in T cells leads to loss of self-tolerance (Suzuki et al., 2001) and enhances the helper function of CD4$^+$ T cells (Soond et al., 2012). However, the results of the studies showed that the *Pten* deficiency drove Th1/Th2-mediated, not Th17-mediated, autoimmunity. Furthermore, recent studies reveal that T reg–specific *Pten* deficiency causes fatal autoimmunity in mice (Huynh et al., 2015; Shrestha et al., 2015). Yet direct evidence showing that *Pten* deficiency leads to T17-mediated autoimmunity by enhancing Akt signaling is lacking, and the relationship between the PTEN/Akt axis and Th17 cells remains elusive. Here, we examined the effect of PTEN on Th17 cells using Th17-specific *Pten*-deficient mice (*Pten*$^{fl/fl}$*Il17a*^{cre}). The data show that deleting *Pten* from Th17 cells induces phosphorylation of Akt and preferentially affects the STAT5 pathway without affecting the mTOR pathway, which explains the increased IL-2 production and subsequent inhibition of Th17 cell differentiation.

We also identified PTEN as a therapeutic target for curing Th17-mediated inflammatory disease. Signaling molecules that play a crucial role in Th17 cell differentiation may be therapeutic targets for inflammatory disease, as reported by recent studies showing that Th17-mediated inflammatory diseases can be cured by treatment with antagonists of IL-6R (Li et al., 2016) and RORγt (Chang et al., 2014). Here, we show that a PTEN inhibitor, SF1670, efficiently blocked Th17 cell differentiation in a dose-dependent manner and ameliorated the symptoms of EAE. SF1670 treatment did not affect cell viability, and periodic treatment with SF1670 did not cause noticeable side effects in mice. In the EAE model, IL-17A

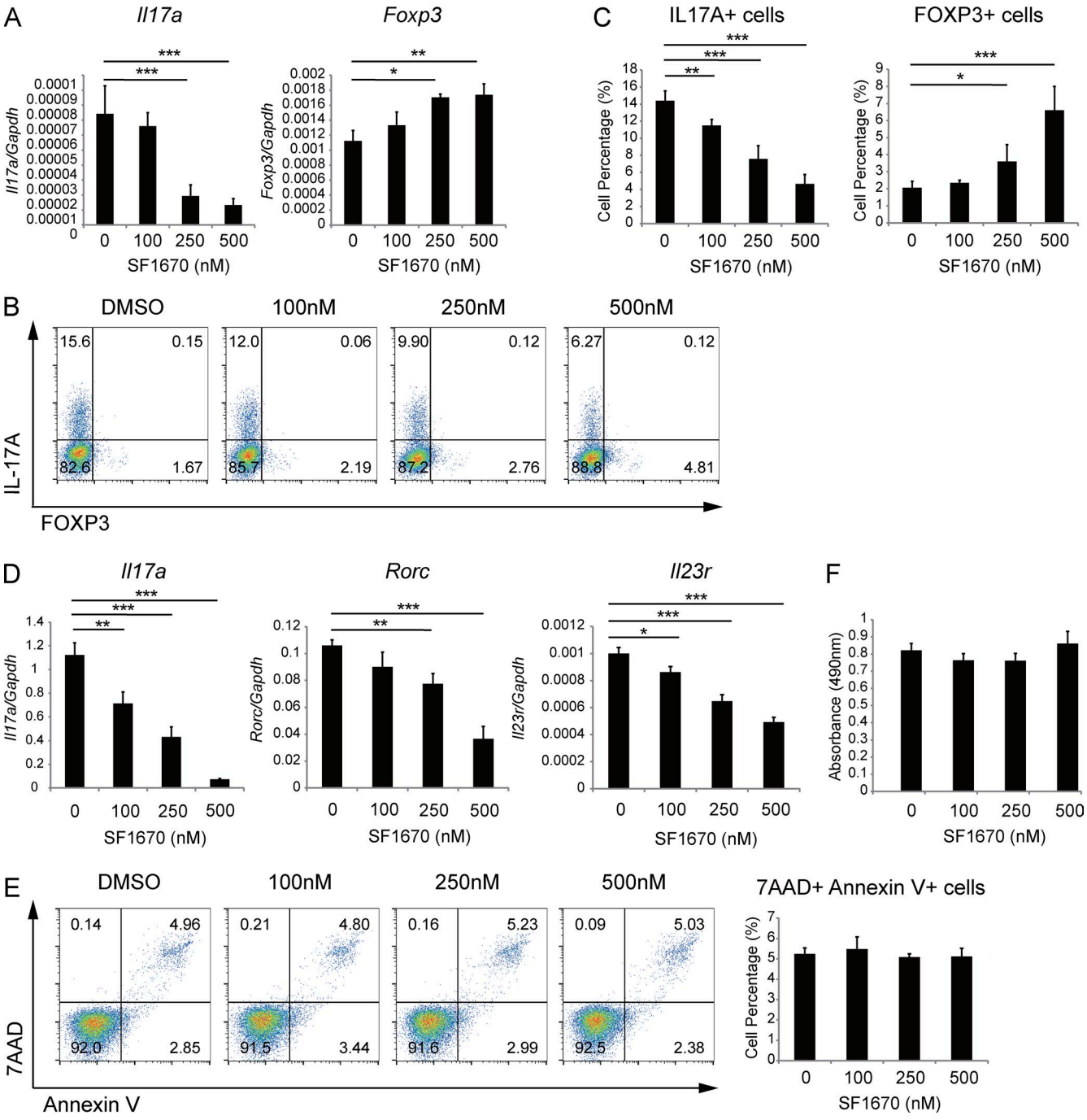

Figure 7. **PTEN inhibitors block Th17 cell differentiation in a dose-dependent manner.** (A) Cells were cultured under Th0-polarizing conditions for 2 d, and *Il17a* and *Foxp3* mRNA levels were measured by qRT-PCR. Data were normalized to *Gapdh* expression. (B and C) Cells were cultured under Th17-polarizing conditions with concomitant treatment with SF1670 as indicated for 3 d. The percentage and number of IL-17A$^+$ and FOXP3$^+$ cells were then measured by flow cytometry. (D) *Il17a*, *Rorc*, and *Il23r* mRNA levels were measured by qRT-PCR. (E and F) Cell viability after treatment with a PTEN inhibitor was measured by flow cytometry (E) and in an MTS assay (F). Data were pooled from three individual experiments (E, right). Data in A, C, D, and F were pooled from three independent experiments. Error bars represent the SD. Statistical differences between groups were determined by the Student *t* test. *, $P < 0.05$; **, $P < 0.01$; and ***, $P < 0.001$.

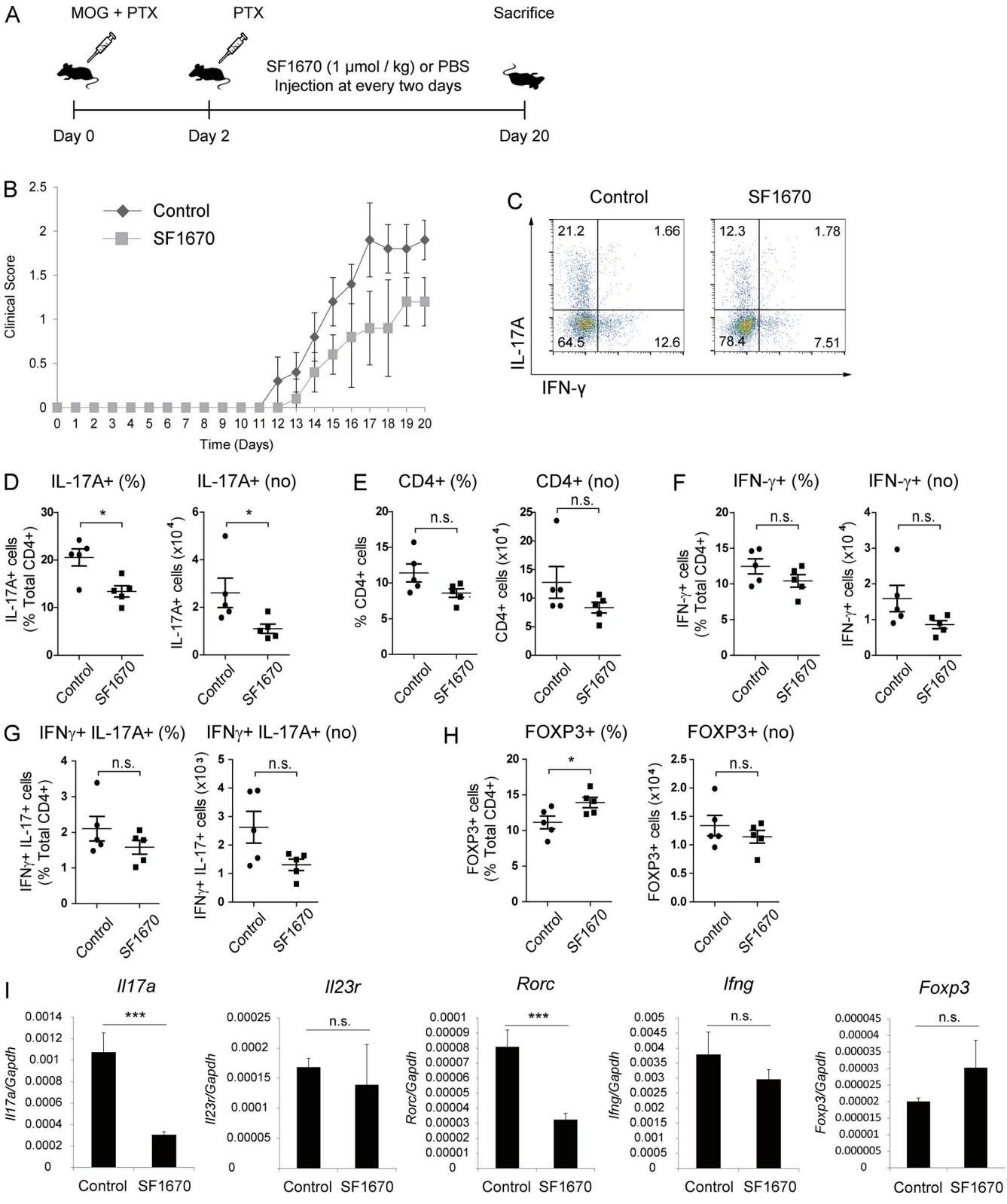

Figure 8. **SF1670 ameliorates the symptoms of EAE by blocking Th17 cell differentiation.** (A) Schematic illustration of EAE induction. EAE was induced as described in the Materials and methods section. PTX, pertussis toxin. (B) The clinical scores for control and SF1670-treated mice (n = 5) after EAE induction. (C) The amount of IFN-γ and IL-17A produced by $CD4^+$ cells from the CNS was measured by flow cytometry. (D–H) Percentage and absolute number (no) of cells infiltrating the CNS. (D) IL-$17A^+$ cells, (E) $CD4^+$ cells, (F) IFN-γ^+ cells, (G) IL-$17A^+$ IFN-γ^+ cells, and (H) $FOXP3^+$ cells. (I) *Il17a*, *Il23r*, *Rorc*,

expression by infiltrating cells was greatly reduced by SF1670, whereas IFN-γ expression showed a small, nonsignificant reduction. The small reduction in the number of IFN-γ^+ cells is likely caused by the reduction in the number of IL-17A$^+$ cells because recent studies show that IL-17A–expressing RORγt^+ T-bet$^+$ cells are converted to IFN-γ–expressing cells (Lee et al., 2009; O'Shea and Paul, 2010; Hirota et al., 2011). In addition, introduction of SF1670 induced FOXP3$^+$ T reg cells, an effect that may be a result of increased IL-2 expression, which acts on the STAT5/FOXP3 axis to induce T reg cell differentiation. Thus, promoting the suppressive function of T reg cells by increasing IL-2 levels may strengthen the effects of SF1670 in ameliorating EAE symptoms. Although we showed that SF1670 ameliorated EAE symptoms, interpretation of the results is somewhat complex and requires caution because the inhibitor may have some off-target effects. Recent studies show that PTEN is essential for T reg cell stability and for their function in suppressing Th1 and Tfh cell responses (Huynh et al., 2015; Shrestha et al., 2015). In addition, PTEN is required for APC-mediated induction of Th17 responses (Blüml et al., 2015; Sahin et al., 2015). SF1670 may affect PTEN activity in non–IL-17A producer cells to reduce EAE severity. Although our experiments on the effect of SF1670 on EAE severity in IL-17A–specific *Pten*-deficient mice suggest that the inhibitor mainly affects IL-17A$^+$ cells (at least under these conditions), we cannot completely exclude the possibility that there may be other unknown off-target effects.

In summary, loss of *Pten* inhibits Th17 cell differentiation. Therefore, targeting PTEN might be a therapeutic strategy for curing autoimmune diseases such as multiple sclerosis, psoriasis, and rheumatoid arthritis. The detailed mechanisms underlying the action of PTEN in the setting of autoimmune disease are still to be identified.

MATERIALS AND METHODS

Mice

C57BL/6 mice (6–8 wk old) were purchased from Daehan Bio Link. *Pten*$^{fl/fl}$ and *Il17a*^{cre} mice were purchased from the Jackson Laboratory. All animal experiments were approved by the Sogang University Institutional Animal Care and Use Committee.

Preparation and differentiation of CD4$^+$ T cells in vitro

CD4$^+$ naive T cells were isolated from 6–8-wk-old mice, and naive T cells were purified using the following antibodies: anti-NK1.1 (108712, BioLegend), anti-CD25 (102014, BioLegend), anti-I-A/I-E (107610, BioLegend), anti-CD8a (100716, BioLegend), BioMag goat anti–rat IgG (Qiagen), and BioMag goat anti–mouse IgG (Qiagen) for negative selection; and biotinylated anti-CD62L (104404, BioLegend) and antibiotin microbeads (Miltenyi Biotec) for positive selection. CD4$^+$ naive T cells were activated by plate-bound anti-CD3ε (10 μg/ml) and anti-CD28 (10 μg/ml) antibodies and incubated for 3 d. The following antibodies and cytokines were used to induce differentiation: Th1 cell differentiation: mouse recombinant IL-2 (1 ng/ml, eBioscience), mouse recombinant IL-12 p70 (3.5 ng/ml, eBioscience), and anti–IL-4 antibody (2 μg/ml); Th2 cell differentiation: mouse recombinant IL-2 (1 ng/ml), mouse recombinant IL-4 (5 ng/ml, eBioscience), and an anti–IFN-γ antibody (2 μg/ml); Th17 cell differentiation: mouse recombinant IL-6 (50 ng/ml, eBioscience), human recombinant TGF-β1 (2 ng/ml, eBioscience), mouse recombinant IL-1β (2 ng/ml, eBioscience), mouse recombinant TNF (1 ng/ml, eBioscience), and anti–IFN-γ (2 μg/ml) and anti–IL-4 antibodies (2 μg/ml); and T reg cell differentiation: mouse recombinant IL-2 (1 ng/ml), human recombinant TGF-β1 (5 ng/ml), and anti–IFN-γ (5 ng/ml) and anti–IL-4 antibodies (5 ng/ml). For another Th17 cell differentiation, mouse recombinant IL-6 (50 ng/ml), mouse recombinant IL-1β (2 ng/ml), and mouse recombinant IL-23 (5 ng/ml, BioLegend) cytokines were used. SF1670 and bpv(phen) (PTEN inhibitors) were purchased from Sigma-Aldrich. A STAT5 inhibitor was purchased from Merck Millipore.

Flow cytometry

Cells were harvested and stimulated for 4 h with PMA (50 ng/ml), ionomycin (750 ng/ml), and Brefeldin A (BioLegend). For intracellular staining, cells were fixed and permeabilized (eBioscience) and then stained with FITC-conjugated anti–IFN-γ (505806, BioLegend), PE-conjugated anti–IL-13 (12-7133-81, eBioscience), PerCP/Cy5.5-conjugated anti–IL-17A (506919, BioLegend), and APC-conjugated anti-FOXP3 (17-5773-80, eBioscience) antibodies. To analyze lymphocyte development in *Pten*$^{fl/fl}$*Il17a*^{cre} mice, cells isolated from the thymus, pLNs, and spleen were stained with FITC-conjugated anti-CD3ε (11-0031-81, eBioscience), PE-conjugated anti-B220 (12-0451-82, eBioscience), PerCP/Cy5.5-conjugated anti-CD8 (126609, BioLegend), APC-conjugated anti-CD4 (100411, BioLegend), FITC-conjugated anti-CD44 (103006, BioLegend), PE-conjugated anti-CD62L (104407, BioLegend), and PerCP/Cy5.5-conjugated anti-TCR γ/δ (118117, BioLegend) antibodies. For other surface antigen staining, cells were stained with APC-conjugated anti–IL-6Rα (115811, BioLegend), APC-conjugated anti-CD45 (103111, BioLegend), FITC-conjugated anti–GR-1 (108405, BioLegend), and FITC-conjugated anti-CD11b (101205, BioLegend) antibodies. Stained cells were then analyzed using a FACSCalibur flow cytometer (BD Bioscience), and data were analyzed with FlowJo software.

Ifng, and *Foxp3* mRNA levels in mononuclear cells from the CNS were measured by qRT-PCR, and data were normalized to *Gapdh* expression. Data in C are representative of five independent experiments, and those in D–I are pooled from five independent experiments. Error bars represent the SD. Statistical differences between groups were determined by the Student *t* test. *, $P < 0.05$; and ***, $P < 0.001$. n.s., not significant.

Phosphorylation analysis

Cells were stimulated with mouse recombinant IL-6 (100 ng/ml, eBioscience) for 15 min at 37°C or with PMA (40 nM) for 15 min at 37°C and then harvested, fixed, and permeabilized in IC Fixation Buffer (eBioscience), and stained with FITC-conjugated anti-pSTAT3 (Y705, 557814, BD Bioscience), FITC-conjugated anti-pSTAT5 (Y694, 11–9010-41, eBioscience), PE-conjugated anti-pAkt (T308, 558275, BD Bioscience), PE-conjugated anti-pAkt (S473, 560378, BD Bioscience), and PE-conjugated anti-pS6 (S235/S236, 12–9007-41, eBioscience). Stained cells were analyzed using a FACSCalibur flow cytometer (BD Bioscience).

Cell viability assay

Cells were cultured for 3 d, and proliferation was measured using a CellTiter 96 AQueous One Solution Cell Proliferation Assay kit (Promega) according to the manufacturer's instructions.

Luciferase reporter assay

The luciferase assay was performed as described previously (Kim et al., 2016). In brief, a pGL3-*Il2* promoter vector, a pRL *Renilla* luciferase control reporter vector, and PTEN siRNA (Santa Cruz Biotechnology, Inc.) were cotransfected into EL4 mouse lymphoma cells using a Gene Pulser (Bio-Rad Laboratories, Inc.) at 950 μF and 270 V. Transfected cells were then allowed to recover in complete medium for 18 h before stimulation with anti-CD3ε (10 μg/ml) and anti-CD28 (10 μg/ml) antibodies for 24 h. Cells were then harvested and examined using the Dual Luciferase Reporter Assay System (Promega), according to the manufacturer's instructions. Relative luciferase activity was calculated by dividing *Firefly* luciferase activity by *Renilla* luciferase activity.

Induction of EAE

At day 0, 8–10-wk-old female mice were immunized subcutaneously with 200 μg of $MOG_{35–55}$ (Peptron) emulsified with CFA containing 5 mg/ml heat-killed *Mycobacterium tuberculosis* (Chondrex), followed by an intraperitoneal injection of 200 ng of pertussis toxin (List Biological Laboratories). Mice then received an intraperitoneal injection of 200 ng of pertussis toxin on day 2. Mice were examined daily for clinical signs of disease, which were scored as follows: 0, no symptoms; 1, limp tail; 2, weakness of hind legs; 3, complete paralysis of hind legs; 4, complete hind leg and partial front leg paralysis; 5, moribund state (Lee et al., 2015).

Isolation and analysis of CNS cells

Mice were anesthetized and perfused. The brain and spinal cord were then removed and homogenized. Mononuclear cells were isolated by gradient centrifugation at 670 *g* for 30 min on a 30/70% Percoll gradient (GE Healthcare). Isolated cells were stimulated with PMA (50 ng/ml), ionomycin (750 ng/ml), and Brefeldin A (BioLegend) for 4 h and then stained with FITC-conjugated anti–IFN-γ (BioLegend), PerCP/Cy5.5-conjugated anti–IL-17A (BioLegend), FITC-conjugated anti–GM-CSF (505403, BioLegend), APC-conjugated anti-FOXP3 (eBioscience), and APC-conjugated anti-CD4 antibodies (Lee et al., 2015).

Isolation of lamina propria lymphocytes

Mice were sacrificed, and intestines were removed, opened longitudinally, and cut into 1cm pieces. The pieces were then incubated twice in 5 mM EDTA in PBS for 15 min at 37°C, and then the epithelial cell layer was removed by vortexing and passing through a 100-μm cell strainer. After incubation with EDTA solution, tissues were washed, minced into small pieces, and digested for 1 h at 37°C in digestion solution containing 4% FBS, 0.5 mg/ml collagenase D (Roche), 0.5 mg/ml DNase I (Sigma-Aldrich), and 3 mg/ml dispase II (Sigma-Aldrich). The resulting solution was strongly vortexed and passed through a 40-μm cell strainer. Mononuclear cells were isolated by gradient centrifugation on a 30/70% Percoll gradient (GE Healthcare) at 670 *g* for 30 min. Isolated cells were stained for ILC3 isolation or stimulated with PMA (50 ng/ml), ionomycin (750 ng/ml), and Brefeldin A (BioLegend) for 4 h and then stained with PerCP/Cy5.5-conjugated IL-17A, and APC-conjugated anti-CD4 antibodies. For ILC3 isolation, cells were stained with FITC-conjugated anti-Lineage cocktail, APC-conjugated anti-CD117, and PerCP/Cy5.5-conjugated anti-NKp46 antibodies, and then $Lineage^{-}$ $NKp46^{-}$ $CD117^{+}$ cells were sorted. All fluorochrome-conjugated antibodies were purchased from BioLegend.

RNA isolation and qRT-PCR

Cells were harvested and homogenized in TRI Reagent (Molecular Research Center, Inc.). Total RNA was isolated according to the manufacturer's instructions, and RT was performed using TOPscript RT (Enzynomics), according to the manufacturer's instructions. qRT-PCR was performed using HiFast Probe Lo-ROX and HiFast SYBR Lo-ROX master mix (PCR Biosystems Ltd.) and a 7500 Real-Time PCR System (Applied Biosystems), according to the manufacturer's instructions. The primers used are listed in Table S1.

Transfection of retroviral shRNA

Pten-shRNA vectors were constructed on a MSCV-LMP backbone (GE Healthcare). Template 97-mer oligonucleotides for *Pten* shRNA were amplified and inserted into the MSCV-LMP vector according to the manufacturer's instructions. The following oligonucleotide sequences were used: shRNA 1, 5′-TGCTGTTGACAGTGAGCGCACAATCTATGTGCTGAGAGACTAGTGAAGCCACAGATGTAGTCTCTCAGCACATAGATTGTATGCCTACTGCCTCGGA-3′; shRNA 2, 5′-TGCTGTTGACAGTGAGCGAACAATGAACCTGATCATTATATAGTGAAGCCACAGATGTATATAATGATCAGGTTCATTGTCTGCCTACTGCCTCGGA-3′; and shRNA 3, 5′-TGCTGTTGACAGTGAGCGCTCTGTGAAGATCTTGACCAATTAGTGAAGCCACAGATGTAATTGGTCAAGATCT-TCACAGAATGCCTACTGCCTCGGA-3′.

ELISA

ELISA was performed as previously described (Kim et al., 2015). In brief, cells were cultured, the supernatant was harvested, and the amount of IL-2 was measured using the following antibodies and reagents: a purified anti–IL-2 antibody (BD Bioscience), a biotin-conjugated anti–IL-2 antibody (BD Bioscience), and mouse recombinant IL-2 (eBioscience). Absorbance was measured at 490 nm in a microplate reader (Bio-Rad).

Microarray analysis

The Affymetrix Whole-Transcript expression array process was executed according to the manufacturer's protocol (GeneChip Whole Transcript PLUS Reagent kit). cDNA was synthesized using the GeneChip Whole Transcript Amplification kit as described by the manufacturer. The sense cDNA was then fragmented and biotin-labeled with terminal deoxynucleotidyl transferase using the GeneChip Whole Transcript Terminal labeling kit. Approximately 5.5 μg of labeled DNA target was hybridized to the Affymetrix GeneChip Mouse 2.0 ST Array at 45°C for 16 h. Hybridized arrays were washed and stained on a GeneChip Fluidics Station 450 and scanned on a GCS3000 Scanner (Affymetrix). Signal values were computed using the Affymetrix GeneChip Command Console software. Raw data were extracted automatically in Affymetrix data extraction protocol using the Command Console Software. After importing CEL files, the data were summarized and normalized with the robust multi-average (RMA) method implemented in Affymetrix Expression Console Software. We exported the result with gene level RMA analysis and performed the differentially expressed gene (DEG) analysis. The comparative analysis between test sample and control sample was performed using fold change. Gene-Enrichment and Functional Annotation analysis for significant probe list was performed using DAVID (http://david.abcc.ncifcrf.gov/home.jsp). All statistical tests and visualizations of differentially expressed genes were conducted using R statistical language v. 3.1.2. (http://www.r-project.org).

Statistical analysis

Data are expressed as the mean ± SD. Differences between groups were determined by Student *t* test. P-values < 0.05 were considered statistically significant (*, $P < 0.05$; **, $P < 0.01$; and ***, $P < 0.001$).

Online supplemental material

Fig. S1 shows development of various lymphocytes in *Pten* conditional KO (cKO) mice. Fig. S2 shows analysis of Th17 using Th17 specific-CRE expressing naive $CD4^+$ T cells or another Th17 polarizing condition in vitro. Fig. S3 shows FOXP3 expression in SF1670-treated induced T reg cells in vitro. Fig. S4 shows analysis of bpv(phen)-treated Th17 cells in vitro. Fig. S5 shows CNS infiltrated cells in SF1670-treated mice and clinical scores for control and SF1670-treated *Pten* cKO mice in which EAE was induced. Table S1 lists the primers used for qRT-PCR. Dataset S1, include as an Excel file, shows gene expression profiles in WT and *Pten* cKO induced T reg cells.

ACKNOWLEDGMENTS

This work was supported by National Research Foundation of Korea grants funded by the South Korean government (NRF-2014R1A2A1A11052545, NRF-2017R1A2B3008621, and NRF-2015M3C9A2054020).

The authors declare no competing financial interests.

Author contributions: H.S. Kim and G.R. Lee designed and analyzed the experiments. H.S. Kim performed most of the experiments. S.W. Jang, W. Lee, K. Kim, H. Sohn, and S.S. Hwang helped with experiments. H.S. Kim wrote the manuscript, and G.R. Lee edited the manuscript. G.R. Lee supervised the study.

Submitted: 22 March 2017

Revised: 14 July 2017

Accepted: 14 August 2017

REFERENCES

Annunziato, F., L. Cosmi, V. Santarlasci, L. Maggi, F. Liotta, B. Mazzinghi, E. Parente, L. Filì, S. Ferri, F. Frosali, et al. 2007. Phenotypic and functional features of human Th17 cells. *J. Exp. Med.* 204:1849–1861. https://doi.org/10.1084/jem.20070663

Bettelli, E., Y. Carrier, W. Gao, T. Korn, T.B. Strom, M. Oukka, H.L. Weiner, and V.K. Kuchroo. 2006. Reciprocal developmental pathways for the generation of pathogenic effector TH17 and regulatory T cells. *Nature.* 441:235–238. https://doi.org/10.1038/nature04753

Blüml, S., E. Sahin, V. Saferding, E. Goncalves-Alves, E. Hainzl, B. Niederreiter, A. Hladik, T. Lohmeyer, J.S. Brunner, M. Bonelli, et al. 2015. Phosphatase and tensin homolog (PTEN) in antigen-presenting cells controls Th17-mediated autoimmune arthritis. *Arthritis Res. Ther.* 17:230. https://doi.org/10.1186/s13075-015-0742-y

Bouguermouh, S., G. Fortin, N. Baba, M. Rubio, and M. Sarfati. 2009. CD28 co-stimulation down regulates Th17 development. *PLoS One.* 4:e5087. https://doi.org/10.1371/journal.pone.0005087

Boyman, O., and J. Sprent. 2012. The role of interleukin-2 during homeostasis and activation of the immune system. *Nat. Rev. Immunol.* 12:180–190. https://doi.org/10.1038/nri3156

Chabaud, M., E. Lubberts, L. Joosten, W. van Den Berg, and P. Miossec. 2001. IL-17 derived from juxta-articular bone and synovium contributes to joint degradation in rheumatoid arthritis. *Arthritis Res.* 3:168–177. https://doi.org/10.1186/ar294

Chang, M.R., B. Lyda, T.M. Kamenecka, and P.R. Griffin. 2014. Pharmacologic repression of retinoic acid receptor-related orphan nuclear receptor γ is therapeutic in the collagen-induced arthritis experimental model. *Arthritis Rheumatol.* 66:579–588. https://doi.org/10.1002/art.38272

Chung, Y., S.H. Chang, G.J. Martinez, X.O. Yang, R. Nurieva, H.S. Kang, L. Ma, S.S. Watowich, A.M. Jetten, Q. Tian, and C. Dong. 2009. Critical regulation of early Th17 cell differentiation by interleukin-1 signaling. *Immunity.* 30:576–587. https://doi.org/10.1016/j.immuni.2009.02.007

Cua, D.J., J. Sherlock, Y. Chen, C.A. Murphy, B. Joyce, B. Seymour, L. Lucian, W. To, S. Kwan, T. Churakova, et al. 2003. Interleukin-23 rather than interleukin-12 is the critical cytokine for autoimmune inflammation of the brain. *Nature.* 421:744–748. https://doi.org/10.1038/nature01355

Decker, E.L., C. Skerka, and P.F. Zipfel. 1998. The early growth response protein (EGR-1) regulates interleukin-2 transcription by synergistic interaction with the nuclear factor of activated T cells. *J. Biol. Chem.* 273:26923–26930. https://doi.org/10.1074/jbc.273.41.26923

de la Iglesia, N., G. Konopka, K.L. Lim, C.L. Nutt, J.F. Bromberg, D.A. Frank, P.S. Mischel, D.N. Louis, and A. Bonni. 2008a. Deregulation of a STAT3-

interleukin 8 signaling pathway promotes human glioblastoma cell proliferation and invasiveness. *J. Neurosci.* 28:5870–5878. https://doi.org/10.1523/JNEUROSCI.5385-07.2008

de la Iglesia, N., G. Konopka, S.V. Puram, J.A. Chan, R.M. Bachoo, M.J. You, D.E. Levy, R.A. Depinho, and A. Bonni. 2008b. Identification of a PTEN-regulated STAT3 brain tumor suppressor pathway. *Genes Dev.* 22:449–462. https://doi.org/10.1101/gad.1606508

Di Cristofano, A., P. Kotsi, Y.F. Peng, C. Cordon-Cardo, K.B. Elkon, and P.P. Pandolfi. 1999. Impaired Fas response and autoimmunity in Pten+/- mice. *Science.* 285:2122–2125. https://doi.org/10.1126/science.285.5436.2122

Eder, A.M., L. Dominguez, T.F. Franke, and J.D. Ashwell. 1998. Phosphoinositide 3-kinase regulation of T cell receptor-mediated interleukin-2 gene expression in normal T cells. *J. Biol. Chem.* 273:28025–28031. https://doi.org/10.1074/jbc.273.43.28025

Elias, K.M., A. Laurence, T.S. Davidson, G. Stephens, Y. Kanno, E.M. Shevach, and J.J. O'Shea. 2008. Retinoic acid inhibits Th17 polarization and enhances FoxP3 expression through a Stat-3/Stat-5 independent signaling pathway. *Blood.* 111:1013–1020. https://doi.org/10.1182/blood-2007-06-096438

Fresno Vara, J.A., E. Casado, J. de Castro, P. Cejas, C. Belda-Iniesta, and M. González-Barón. 2004. PI3K/Akt signalling pathway and cancer. *Cancer Treat. Rev.* 30:193–204. https://doi.org/10.1016/j.ctrv.2003.07.007

Fung, M.M., F. Rohwer, and K.L. McGuire. 2003. IL-2 activation of a PI3K-dependent STAT3 serine phosphorylation pathway in primary human T cells. *Cell. Signal.* 15:625–636. https://doi.org/10.1016/S0898-6568(03)00003-2

Gaffen, S.L. 2001. Signaling domains of the interleukin 2 receptor. *Cytokine.* 14:63–77. https://doi.org/10.1006/cyto.2001.0862

Ghoreschi, K., A. Laurence, X.P. Yang, C.M. Tato, M.J. McGeachy, J.E. Konkel, H.L. Ramos, L. Wei, T.S. Davidson, N. Bouladoux, et al. 2010. Generation of pathogenic T(H)17 cells in the absence of TGF-β signalling. *Nature.* 467:967–971. https://doi.org/10.1038/nature09447

Hirota, K., J.H. Duarte, M. Veldhoen, E. Hornsby, Y. Li, D.J. Cua, H. Ahlfors, C. Wilhelm, M. Tolaini, U. Menzel, et al. 2011. Fate mapping of IL-17-producing T cells in inflammatory responses. *Nat. Immunol.* 12:255–263. https://doi.org/10.1038/ni.1993

Huynh, A., M. DuPage, B. Priyadharshini, P.T. Sage, J. Quiros, C.M. Borges, N. Townamchai, V.A. Gerriets, J.C. Rathmell, A.H. Sharpe, et al. 2015. Control of PI(3) kinase in Treg cells maintains homeostasis and lineage stability. *Nat. Immunol.* 16:188–196. https://doi.org/10.1038/ni.3077

Ivanov, I.I., B.S. McKenzie, L. Zhou, C.E. Tadokoro, A. Lepelley, J.J. Lafaille, D.J. Cua, and D.R. Littman. 2006. The orphan nuclear receptor RORgammat directs the differentiation program of proinflammatory IL-17+ T helper cells. *Cell.* 126:1121–1133. https://doi.org/10.1016/j.cell.2006.07.035

June, C.H., J.A. Ledbetter, M.M. Gillespie, T. Lindsten, and C.B. Thompson. 1987. T-cell proliferation involving the CD28 pathway is associated with cyclosporine-resistant interleukin 2 gene expression. *Mol. Cell. Biol.* 7:4472–4481. https://doi.org/10.1128/MCB.7.12.4472

Kane, L.P., V.S. Shapiro, D. Stokoe, and A. Weiss. 1999. Induction of NF-kappaB by the Akt/PKB kinase. *Curr. Biol.* 9:601–604. https://doi.org/10.1016/S0960-9822(99)80265-6

Kane, L.P., P.G. Andres, K.C. Howland, A.K. Abbas, and A. Weiss. 2001. Akt provides the CD28 costimulatory signal for up-regulation of IL-2 and IFN-gamma but not TH2 cytokines. *Nat. Immunol.* 2:37–44. https://doi.org/10.1038/83144

Kim, H.P., J. Imbert, and W.J. Leonard. 2006. Both integrated and differential regulation of components of the IL-2/IL-2 receptor system. *Cytokine Growth Factor Rev.* 17:349–366. https://doi.org/10.1016/j.cytogfr.2006.07.003

Kim, K., N.J. Kim, S.Y. Kim, I.H. Kim, K.S. Kim, and G.R. Lee. 2015. Cyclo(Phe-Pro) produced by the human pathogen Vibrio vulnificus inhibits host innate immune responses through the NF-κB pathway. *Infect. Immun.* 83:1150–1161. https://doi.org/10.1128/IAI.02878-14

Kim, K., N. Kim, and G.R. Lee. 2016. Transcription Factors Oct-1 and GATA-3 Cooperatively Regulate Th2 Cytokine Gene Expression via the RHS5 within the Th2 Locus Control Region. *PLoS One.* 11:e0148576. https://doi.org/10.1371/journal.pone.0148576

Kimura, A., and T. Kishimoto. 2010. IL-6: regulator of Treg/Th17 balance. *Eur. J. Immunol.* 40:1830–1835. https://doi.org/10.1002/eji.201040391

Komiyama, Y., S. Nakae, T. Matsuki, A. Nambu, H. Ishigame, S. Kakuta, K. Sudo, and Y. Iwakura. 2006. IL-17 plays an important role in the development of experimental autoimmune encephalomyelitis. *J. Immunol.* 177:566–573. https://doi.org/10.4049/jimmunol.177.1.566

Korn, T., E. Bettelli, M. Oukka, and V.K. Kuchroo. 2009. IL-17 and Th17 Cells. *Annu. Rev. Immunol.* 27:485–517. https://doi.org/10.1146/annurev.immunol.021908.132710

Kumar, P.P., P.K. Purbey, D.S. Ravi, D. Mitra, and S. Galande. 2005. Displacement of SATB1-bound histone deacetylase 1 corepressor by the human immunodeficiency virus type 1 transactivator induces expression of interleukin-2 and its receptor in T cells. *Mol. Cell. Biol.* 25:1620–1633. https://doi.org/10.1128/MCB.25.5.1620-1633.2005

Kurebayashi, Y., S. Nagai, A. Ikejiri, M. Ohtani, K. Ichiyama, Y. Baba, T. Yamada, S. Egami, T. Hoshii, A. Hirao, et al. 2012. PI3K-Akt-mTORC1-S6K1/2 axis controls Th17 differentiation by regulating Gfi1 expression and nuclear translocation of RORγ. *Cell Reports.* 1:360–373. https://doi.org/10.1016/j.celrep.2012.02.007

Laurence, A., C.M. Tato, T.S. Davidson, Y. Kanno, Z. Chen, Z. Yao, R.B. Blank, F. Meylan, R. Siegel, L. Hennighausen, et al. 2007. Interleukin-2 signaling via STAT5 constrains T helper 17 cell generation. *Immunity.* 26:371–381. https://doi.org/10.1016/j.immuni.2007.02.009

Lee, S.H., J.S. Park, J.K. Byun, J. Jhun, K. Jung, H.B. Seo, Y.M. Moon, H.Y. Kim, S.H. Park, and M.L. Cho. 2016. PTEN ameliorates autoimmune arthritis through down-regulating STAT3 activation with reciprocal balance of Th17 and Tregs. *Sci. Rep.* 6:34617. https://doi.org/10.1038/srep34617

Lee, W., H. Su Kim, and G.R. Lee. 2015. Leukotrienes induce the migration of Th17 cells. *Immunol. Cell Biol.* 93:472–479. https://doi.org/10.1038/icb.2014.104

Lee, Y.K., H. Turner, C.L. Maynard, J.R. Oliver, D. Chen, C.O. Elson, and C.T. Weaver. 2009. Late developmental plasticity in the T helper 17 lineage. *Immunity.* 30:92–107. https://doi.org/10.1016/j.immuni.2008.11.005

Lee, Y.K., J.S. Menezes, Y. Umesaki, and S.K. Mazmanian. 2011. Proinflammatory T-cell responses to gut microbiota promote experimental autoimmune encephalomyelitis. *Proc. Natl. Acad. Sci. USA.* 108(Suppl 1):4615–4622. https://doi.org/10.1073/pnas.1000082107

Li, S., Z. Wu, L. Li, and X. Liu. 2016. Interleukin-6 (IL-6) Receptor Antagonist Protects Against Rheumatoid Arthritis. *Med. Sci. Monit.* 22:2113–2118. https://doi.org/10.12659/MSM.896355

Li, Y., A. Prasad, Y. Jia, S.G. Roy, F. Loison, S. Mondal, P. Kocjan, L.E. Silberstein, S. Ding, and H.R. Luo. 2011. Pretreatment with phosphatase and tensin homolog deleted on chromosome 10 (PTEN) inhibitor SF1670 augments the efficacy of granulocyte transfusion in a clinically relevant mouse model. *Blood.* 117:6702–6713. https://doi.org/10.1182/blood-2010-09-309864

Liao, W., J.X. Lin, L. Wang, P. Li, and W.J. Leonard. 2011. Modulation of cytokine receptors by IL-2 broadly regulates differentiation into helper T cell lineages. *Nat. Immunol.* 12:551–559. https://doi.org/10.1038/ni.2030

Lin, J.X., and W.J. Leonard. 2000. The role of Stat5a and Stat5b in signaling by IL-2 family cytokines. *Oncogene.* 19:2566–2576. https://doi.org/10.1038/sj.onc.1203523

Maehama, T., and J.E. Dixon. 1998. The tumor suppressor, PTEN/MMAC1, dephosphorylates the lipid second messenger, phosphatidylinositol 3,4,5-trisphosphate. *J. Biol. Chem.* 273:13375–13378. https://doi.org/10.1074/jbc.273.22.13375

Mangan, P.R., L.E. Harrington, D.B. O'Quinn, W.S. Helms, D.C. Bullard, C.O. Elson, R.D. Hatton, S.M. Wahl, T.R. Schoeb, and C.T. Weaver. 2006. Transforming growth factor-beta induces development of the T(H)17 lineage. *Nature.* 441:231–234. https://doi.org/10.1038/nature04754

Moon, S.H., D.K. Kim, Y. Cha, I. Jeon, J. Song, and K.S. Park. 2013. PI3K/Akt and Stat3 signaling regulated by PTEN control of the cancer stem cell population, proliferation and senescence in a glioblastoma cell line. *Int. J. Oncol.* 42:921–928. https://doi.org/10.3892/ijo.2013.1765

O'Shea, J.J., and W.E. Paul. 2010. Mechanisms underlying lineage commitment and plasticity of helper CD4+ T cells. *Science.* 327:1098–1102. https://doi.org/10.1126/science.1178334

Pierau, M., S. Engelmann, D. Reinhold, T. Lapp, B. Schraven, and U.H. Bommhardt. 2009. Protein kinase B/Akt signals impair Th17 differentiation and support natural regulatory T cell function and induced regulatory T cell formation. *J. Immunol.* 183:6124–6134. https://doi.org/10.4049/jimmunol.0900246

Sahin, E., J.S. Brunner, J.B. Kral, M. Kuttke, L. Hanzl, H. Datler, H. Paar, N. Neuwinger, V. Saferding, E. Zinser, et al. 2015. Loss of Phosphatase and Tensin Homolog in APCs Impedes Th17-Mediated Autoimmune Encephalomyelitis. *J. Immunol.* 195:2560–2570. https://doi.org/10.4049/jimmunol.1402511

Schmid, A.C., R.D. Byrne, R. Vilar, and R. Woscholski. 2004. Bisperoxovanadium compounds are potent PTEN inhibitors. *FEBS Lett.* 566:35–38. https://doi.org/10.1016/j.febslet.2004.03.102

Shrestha, S., K. Yang, C. Guy, P. Vogel, G. Neale, and H. Chi. 2015. Treg cells require the phosphatase PTEN to restrain TH1 and TFH cell responses. *Nat. Immunol.* 16:178–187. https://doi.org/10.1038/ni.3076

Soond, D.R., F. Garçon, D.T. Patton, J. Rolf, M. Turner, C. Scudamore, O.A. Garden, and K. Okkenhaug. 2012. Pten loss in CD4 T cells enhances their helper function but does not lead to autoimmunity or lymphoma. *J. Immunol.* 188:5935–5943. https://doi.org/10.4049/jimmunol.1102116

Stambolic, V., A. Suzuki, J.L. de la Pompa, G.M. Brothers, C. Mirtsos, T. Sasaki, J. Ruland, J.M. Penninger, D.P. Siderovski, and T.W. Mak. 1998. Negative regulation of PKB/Akt-dependent cell survival by the tumor suppressor PTEN. *Cell.* 95:29–39. https://doi.org/10.1016/S0092-8674(00)81780-8

Sun, S., and B.M. Steinberg. 2002. PTEN is a negative regulator of STAT3 activation in human papillomavirus-infected cells. *J. Gen. Virol.* 83:1651–1658. https://doi.org/10.1099/0022-1317-83-7-1651

Suzuki, A., M.T. Yamaguchi, T. Ohteki, T. Sasaki, T. Kaisho, Y. Kimura, R. Yoshida, A. Wakeham, T. Higuchi, M. Fukumoto, et al. 2001. T cell-specific loss of Pten leads to defects in central and peripheral tolerance. *Immunity.* 14:523–534. https://doi.org/10.1016/S1074-7613(01)00134-0

Tenbrock, K., Y.T. Juang, M.F. Gourley, M.P. Nambiar, and G.C. Tsokos. 2002. Antisense cyclic adenosine 5′-monophosphate response element modulator up-regulates IL-2 in T cells from patients with systemic lupus erythematosus. *J. Immunol.* 169:4147–4152. https://doi.org/10.4049/jimmunol.169.8.4147

Tenbrock, K., Y.T. Juang, M. Tolnay, and G.C. Tsokos. 2003. The cyclic adenosine 5′-monophosphate response element modulator suppresses IL-2 production in stimulated T cells by a chromatin-dependent mechanism. *J. Immunol.* 170:2971–2976. https://doi.org/10.4049/jimmunol.170.6.2971

Veldhoen, M., R.J. Hocking, C.J. Atkins, R.M. Locksley, and B. Stockinger. 2006. TGFbeta in the context of an inflammatory cytokine milieu supports de novo differentiation of IL-17-producing T cells. *Immunity.* 24:179–189. https://doi.org/10.1016/j.immuni.2006.01.001

Ward, S.G., S.C. Ley, C. MacPhee, and D.A. Cantrell. 1992. Regulation of D-3 phosphoinositides during T cell activation via the T cell antigen receptor/CD3 complex and CD2 antigens. *Eur. J. Immunol.* 22:45–49. https://doi.org/10.1002/eji.1830220108

Yang, X.O., B.P. Pappu, R. Nurieva, A. Akimzhanov, H.S. Kang, Y. Chung, L. Ma, B. Shah, A.D. Panopoulos, K.S. Schluns, et al. 2008. T helper 17 lineage differentiation is programmed by orphan nuclear receptors ROR alpha and ROR gamma. *Immunity.* 28:29–39. https://doi.org/10.1016/j.immuni.2007.11.016

Yang, X.P., K. Ghoreschi, S.M. Steward-Tharp, J. Rodriguez-Canales, J. Zhu, J.R. Grainger, K. Hirahara, H.W. Sun, L. Wei, G. Vahedi, et al. 2011. Opposing regulation of the locus encoding IL-17 through direct, reciprocal actions of STAT3 and STAT5. *Nat. Immunol.* 12:247–254. https://doi.org/10.1038/ni.1995

Zhou, L., M.M. Chong, and D.R. Littman. 2009. Plasticity of CD4+ T cell lineage differentiation. *Immunity.* 30:646–655. https://doi.org/10.1016/j.immuni.2009.05.001

Zhu, J., H. Yamane, and W.E. Paul. 2010. Differentiation of effector CD4 T cell populations (*). *Annu. Rev. Immunol.* 28:445–489. https://doi.org/10.1146/annurev-immunol-030409-101212